Central and Northern Apennines


APAT
Agenzia per la Protezione dell'Ambiente e per i Servizi Tecnici
Dipartimento Difesa del Suolo
Servizio Geologico d'Italia
GEOLOGICAL MAP OF ITALY
1:1 250 000 Scale
MAIN TECTONO-STRATIGRAPHIC UNITS
SPECIALLY PRINTED FOR THE 32nd INTERNATIONAL GEOLOGICAL CONGRESS
ITALIA 2004

The Apennines

http://eol.jsc.nasa.gov/

ISS004E10538

Central Apennines

http://eol.jsc.nasa.gov/

Avezzano, Central Apennines, east of Rome

Assisi, Central Apennines

San Gimignano, Central Apennines

View from Siena, Central Apennines

ISS014E17038

Sta Margharita, Ligurian Apennines

http://eol.jsc.nasa.gov/

ISS014E17037

Genoa, Ligurian Apennines

http://eol.jsc.nasa.gov/

Ligurian Apennines, north of San Remo

Ligurian inland village

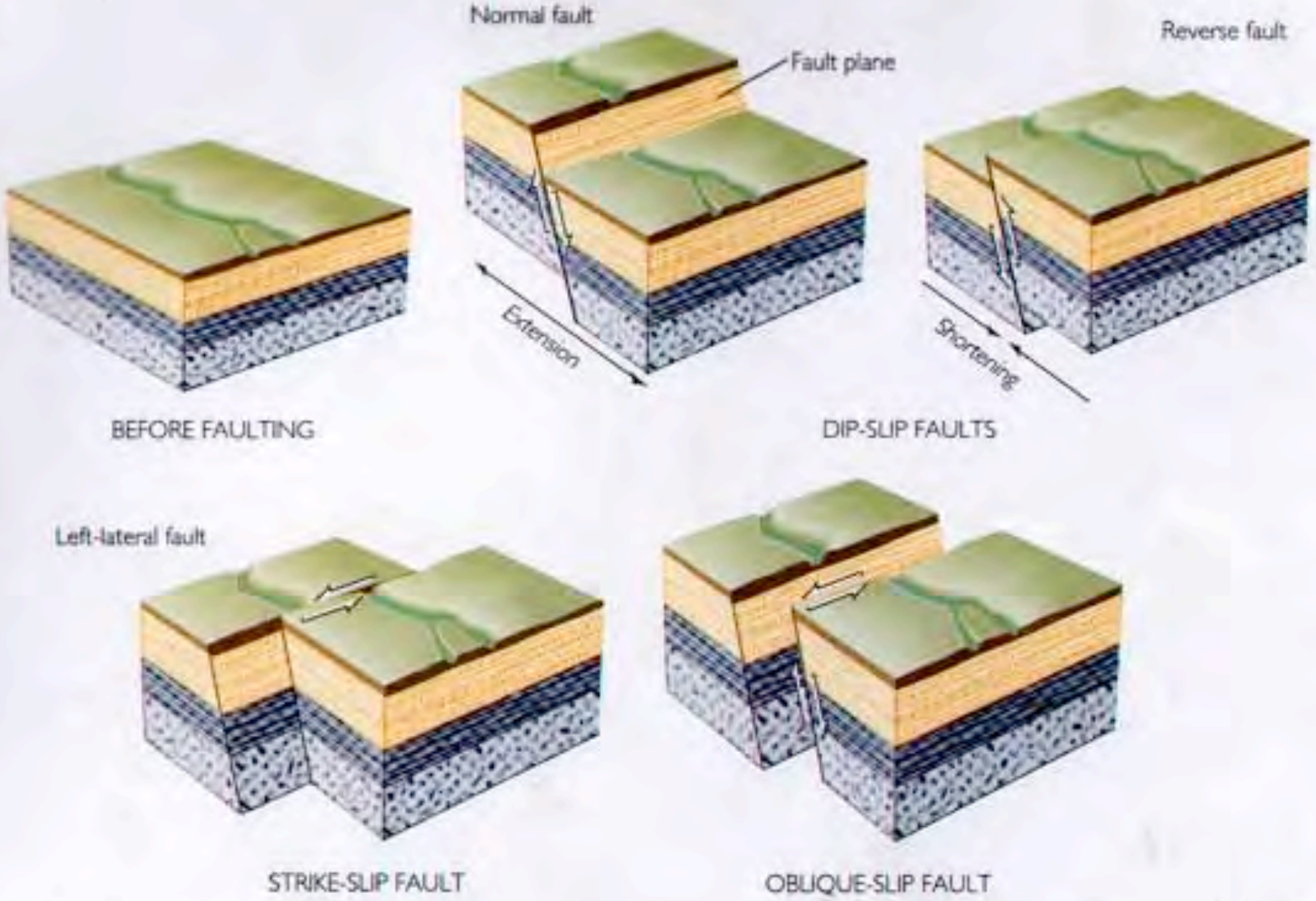

Figure 10.22
Press and Siever: ***Understanding Earth***

OHT 54

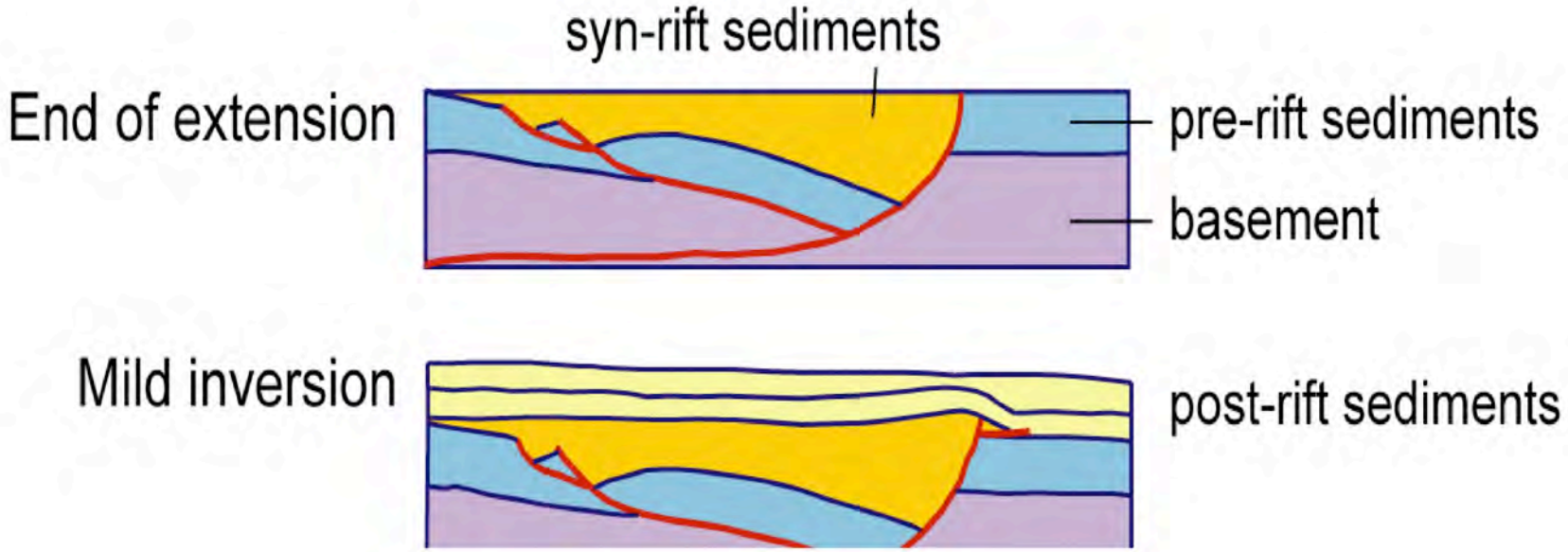

Why do we see marine sediments in the Apennine summits?
Because the basins “invert”. Why?

Because the stresses changes as the Apeninnes grow

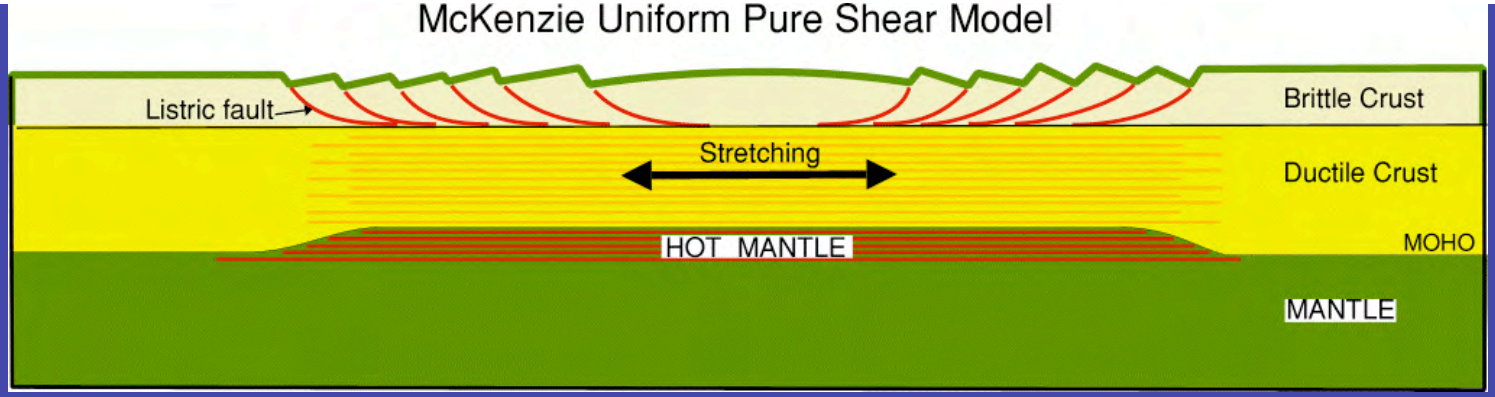

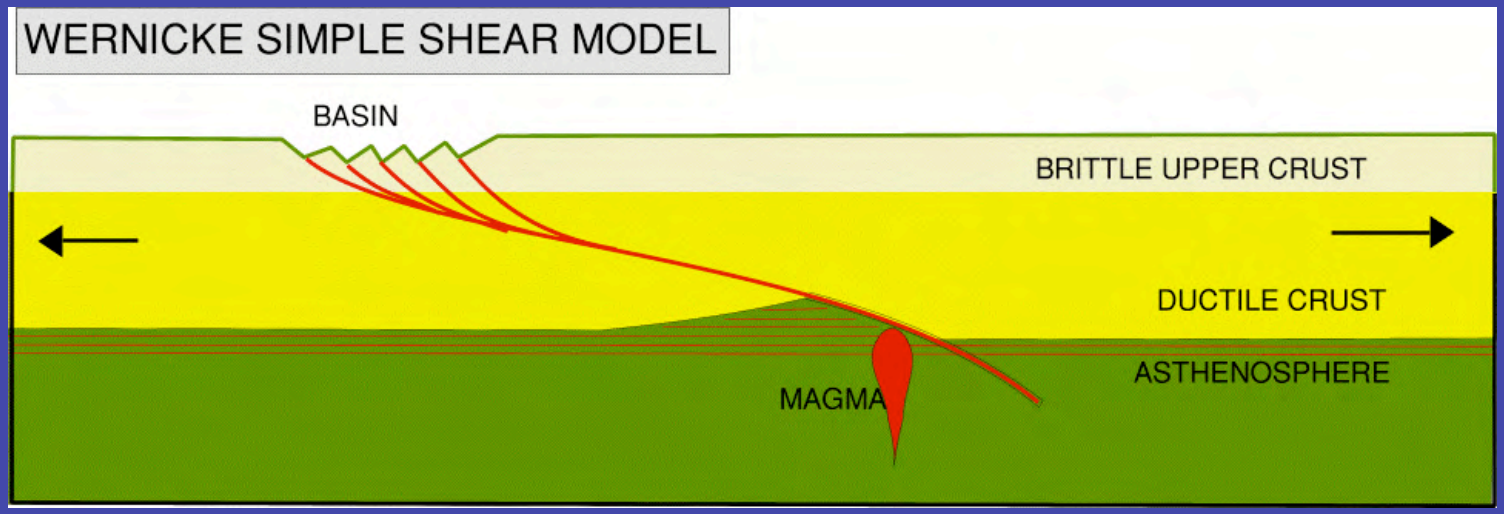

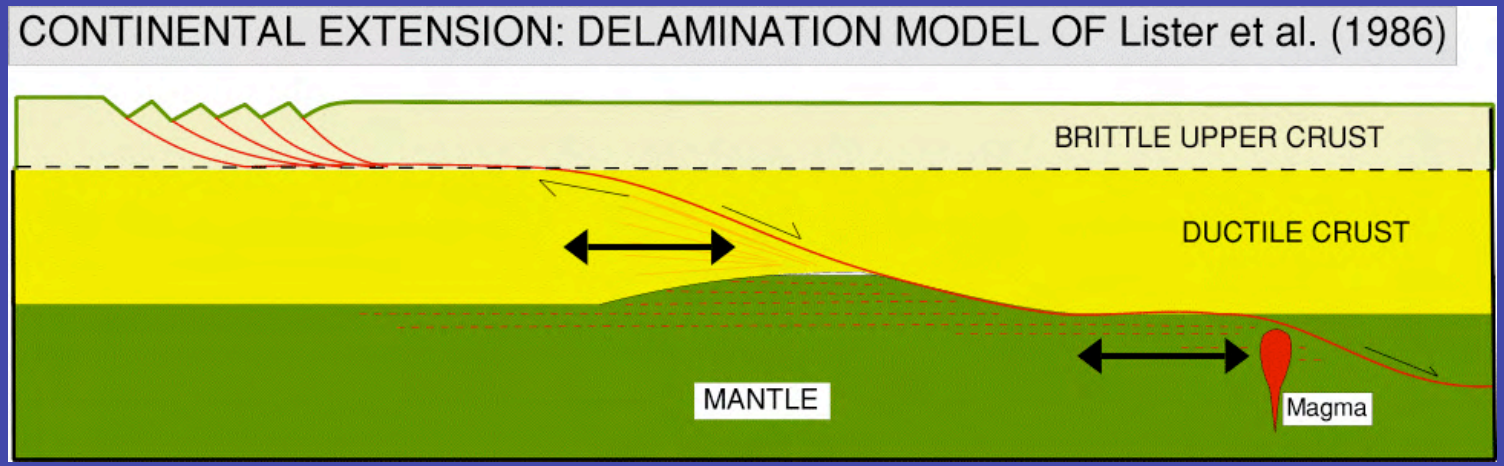

http://www.le.ac.uk/geology/art/gl209/lecture4/lecture4.html

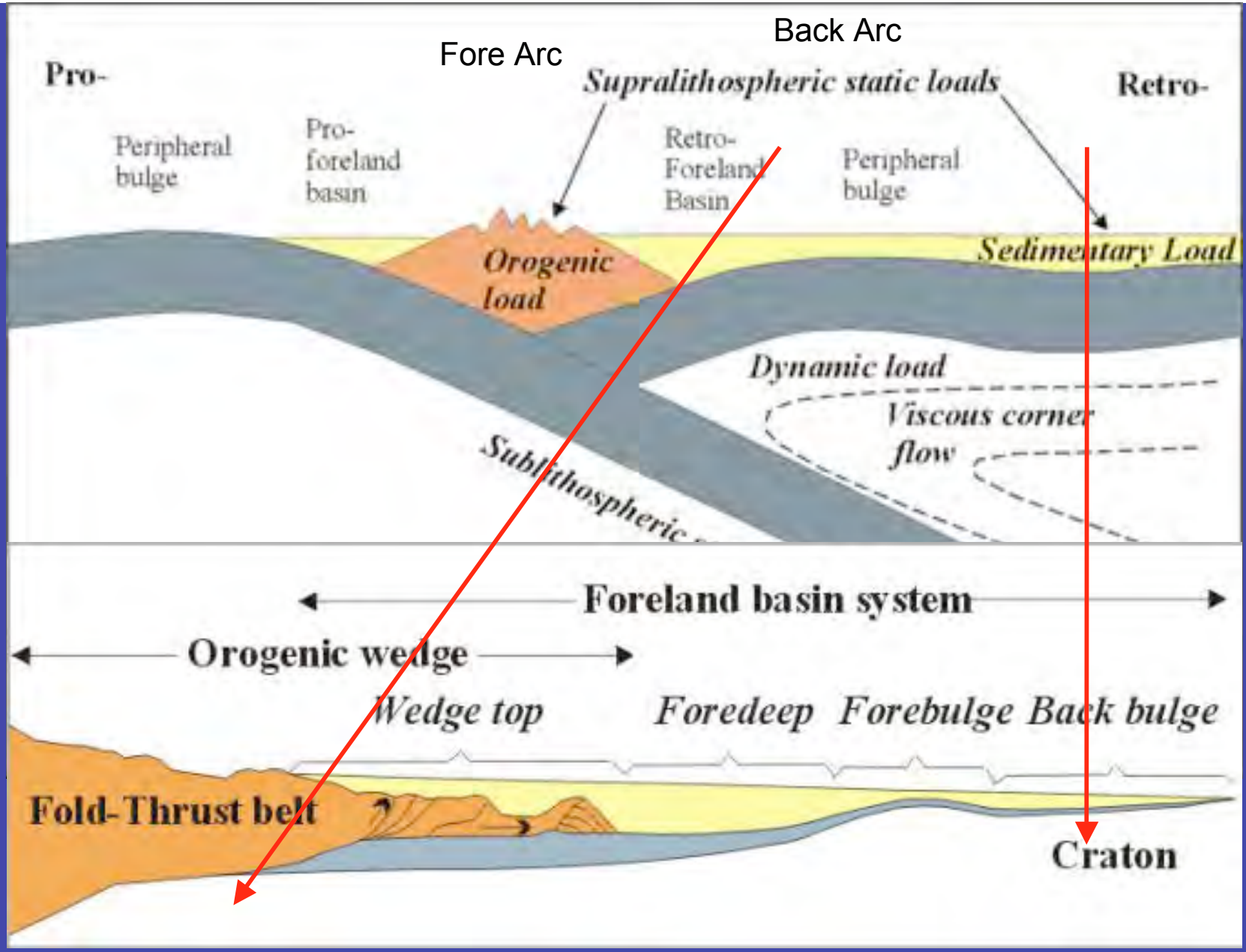

http://manhattan.unipv.it/sedgeo/Research/Basin%20Analysis.htm

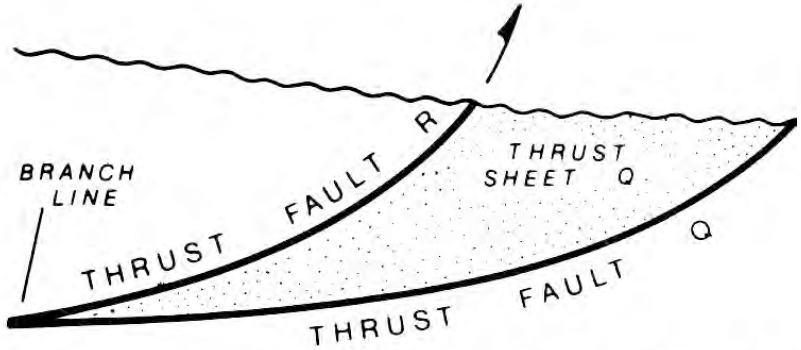

FIG. 1—Cross section through thrust sheet (Q), which is ume of rock above leading fault (Q) and below trailing (R).

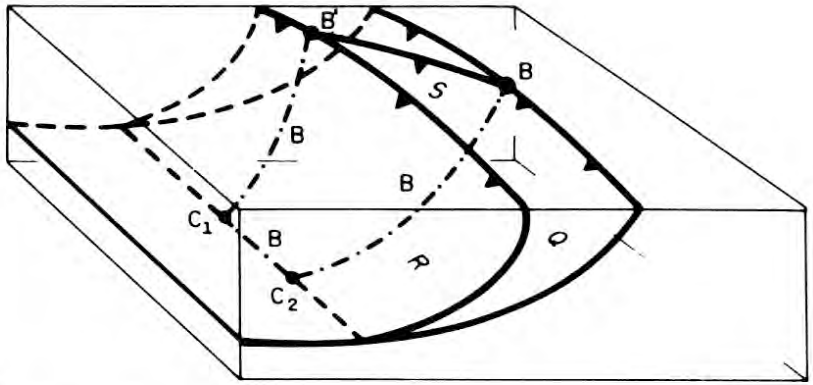

FIG. 7—Two major faults (Q, R) with connecting splay (S). Two branch lines (B) have surface terminations (B, B′) and one branch line at depth has two corners (C_1, C_2).

Boyer and Elliott 1982

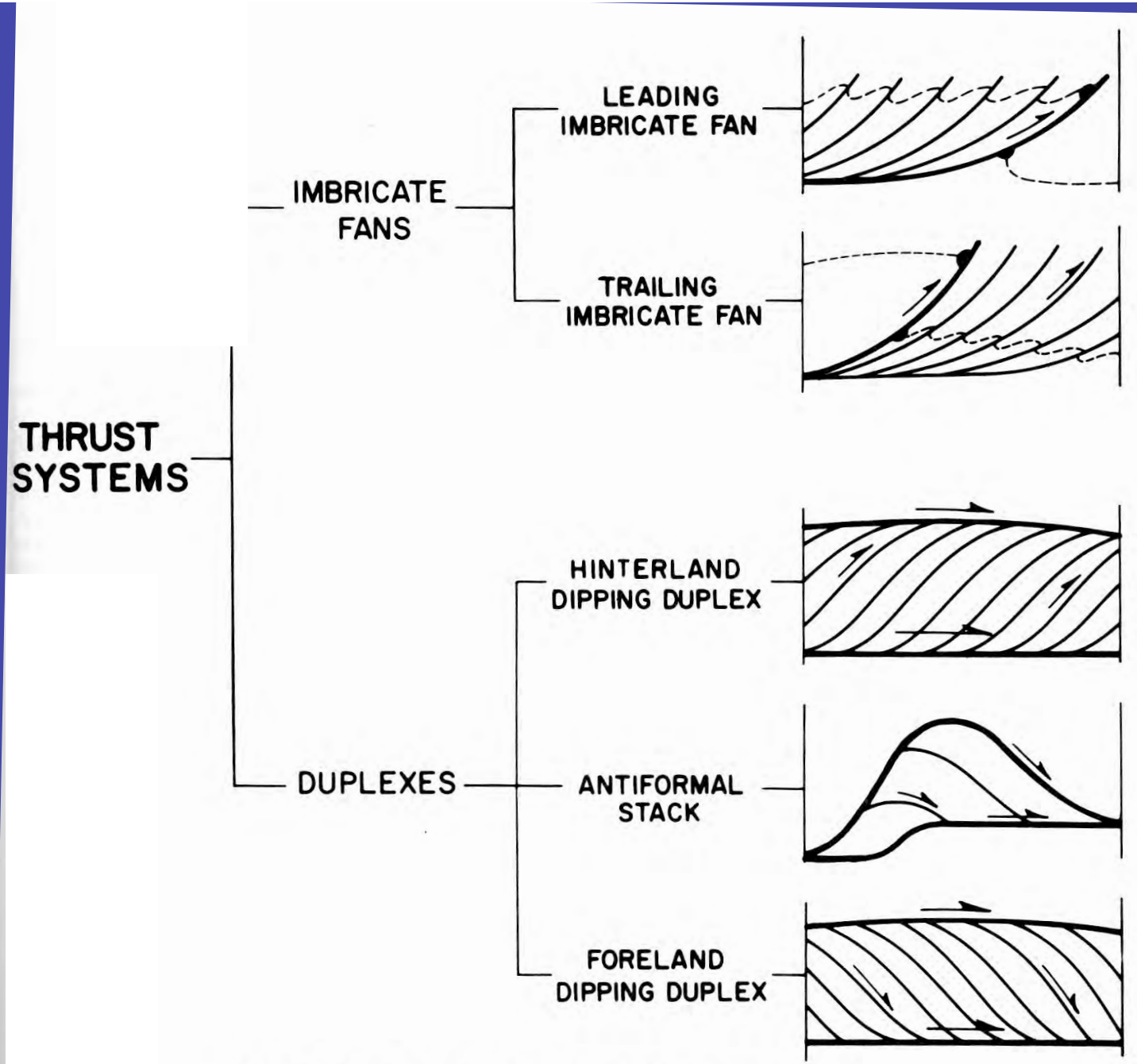

FIG. 12—Classification of different systems of thrusts; most are imbricate.

Boyer and Elliott 1982

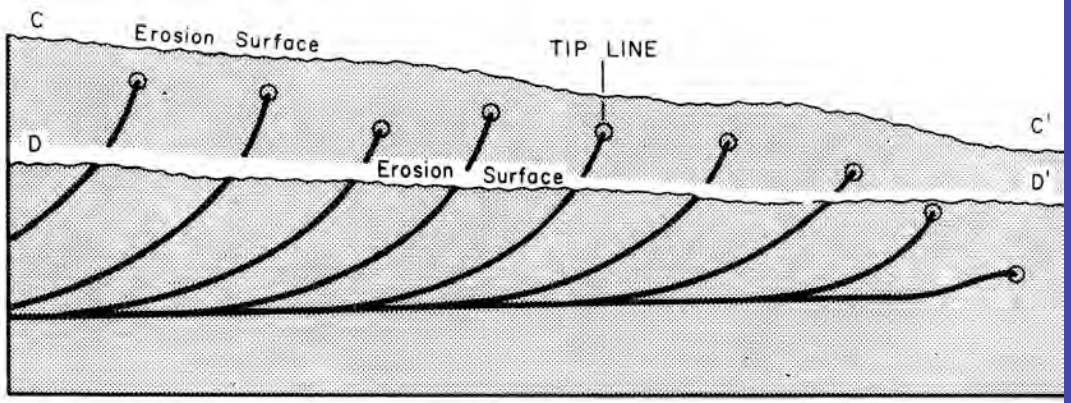

FIG. 11—Cross section of imbricate fan at two different levels of erosion. Each thrust sheet is an upward-opening crescentic slic and all curve asymptotically downward to a common basal sole thrust. If most faults cut synorogenic erosion surface DD′ we ha an emergent imbricate fan. Alternatively, it is possible that tip lines do not reach synorogenic erosion surface CC′, producing blir imbricate fan. Note that subsequent erosion (CC′ down to DD′) may obliterate any means of distinguishing two kinds of imb cate fans.

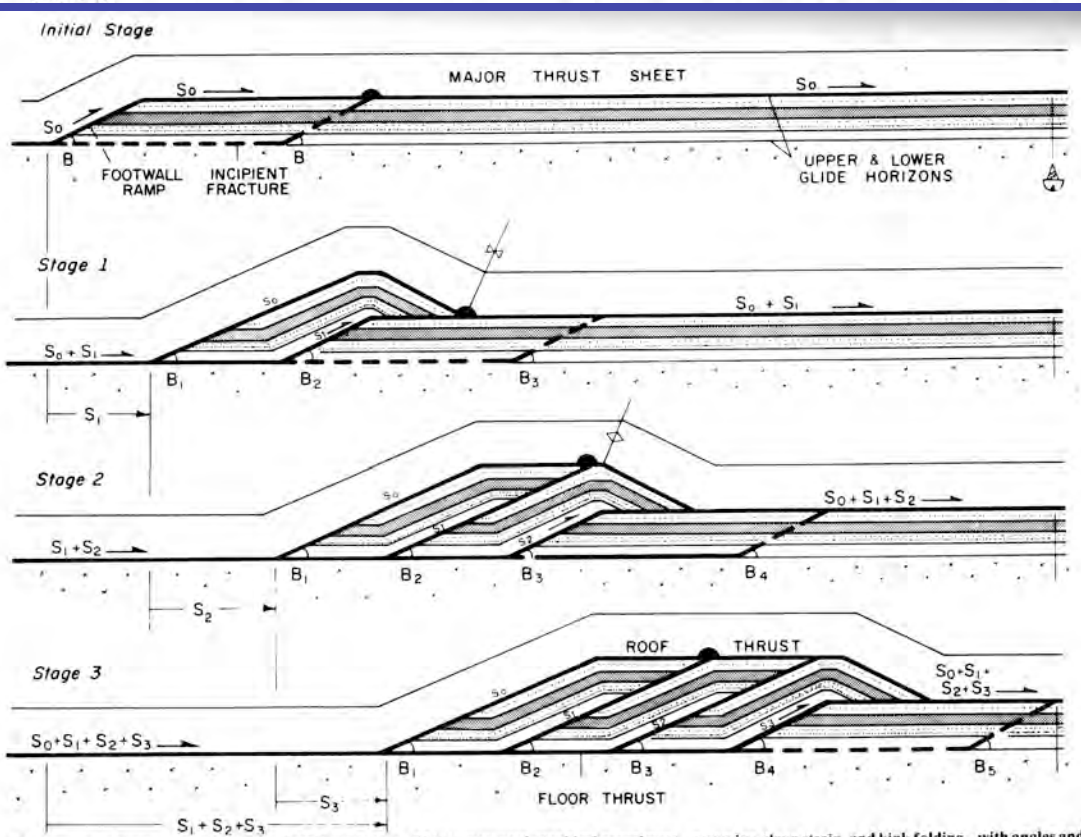

FIG. 19—Progressive collapse of footwall ramp builds up duplex. This is measured graphical experiment, assuming plane strain and kink folding, with angles and ratios of dimensions typical of natural examples (Table 1). Roof thrust sheet undergoes complex sequence of folding and unfolding, seen by following black half dot. Modified from Boyer (1978).

Boyer and Elliott 1982

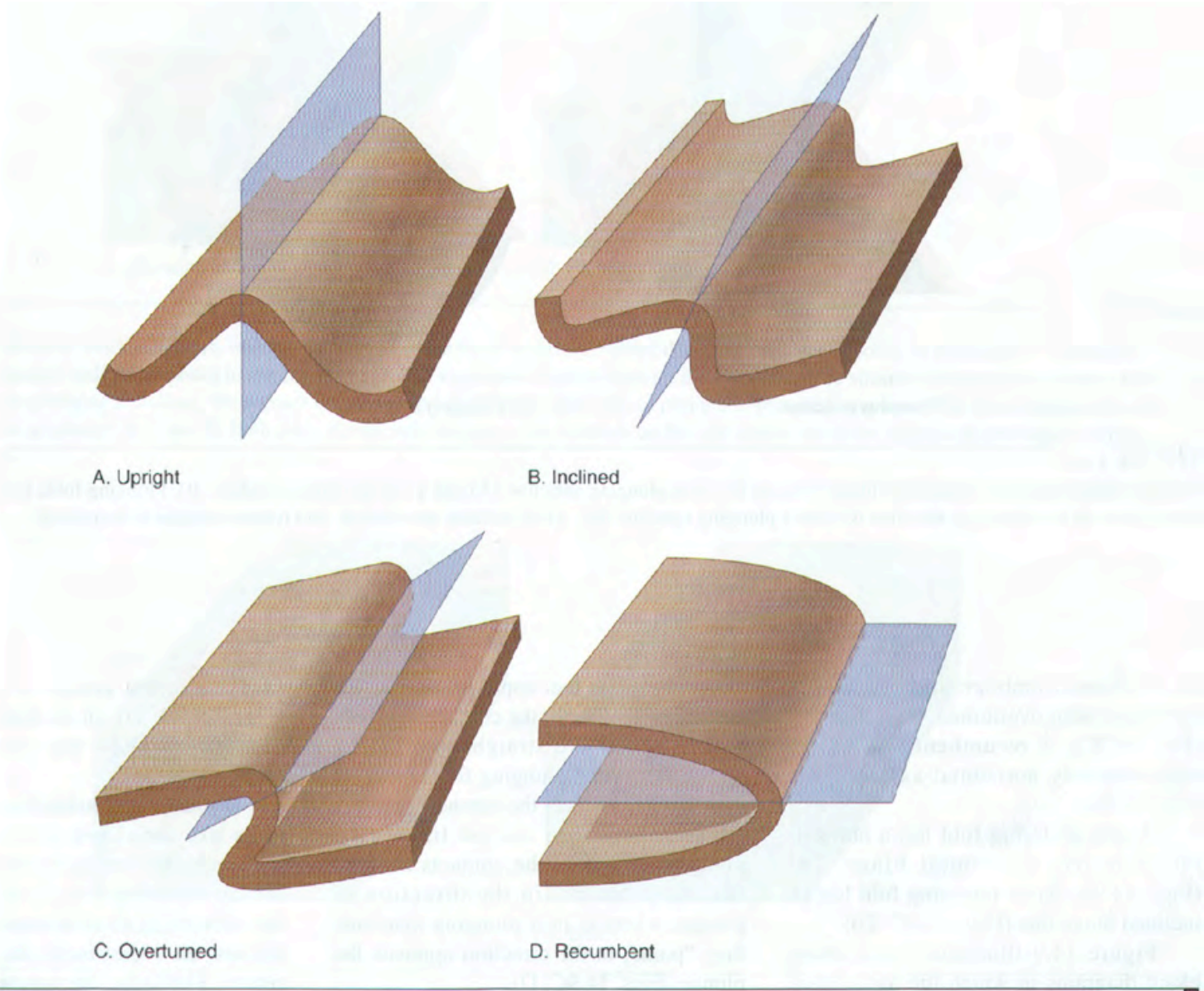

FIGURE 14.7
The axial surface of a fold can be: A. Vertical in **upright folds;** B. inclined in **inclined folds;** C. inclined so much that opposite limbs dip in the same direction in **overturned folds;** D. horizontal in **recumbent folds.** (Adapted from Jones, 2001: Laboratory Manual for Physical Geology, 3rd Edition)

http://www.eas.purdue.edu/mesozoic/Lab_12/Fold_axial_surface_types.jpg

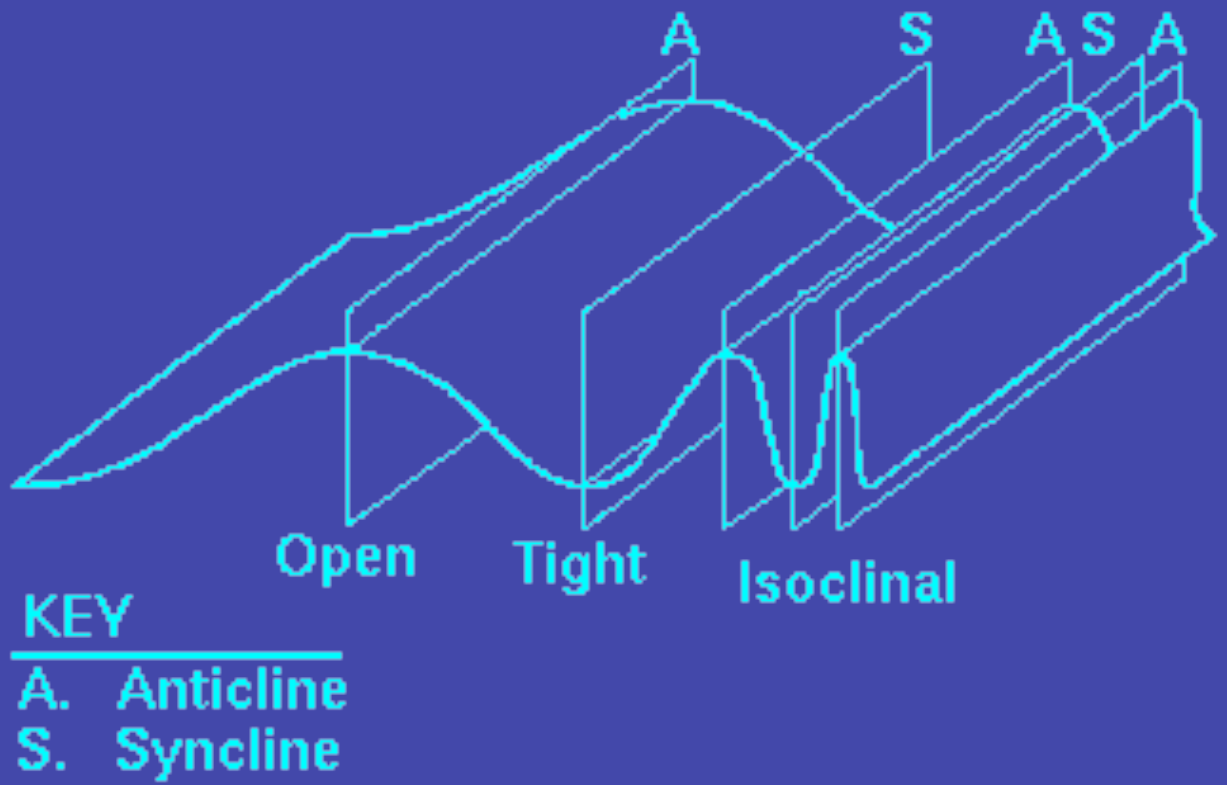

http://homepage.usask.ca/~mjr347/prog/geoe118/geoe118.047.html

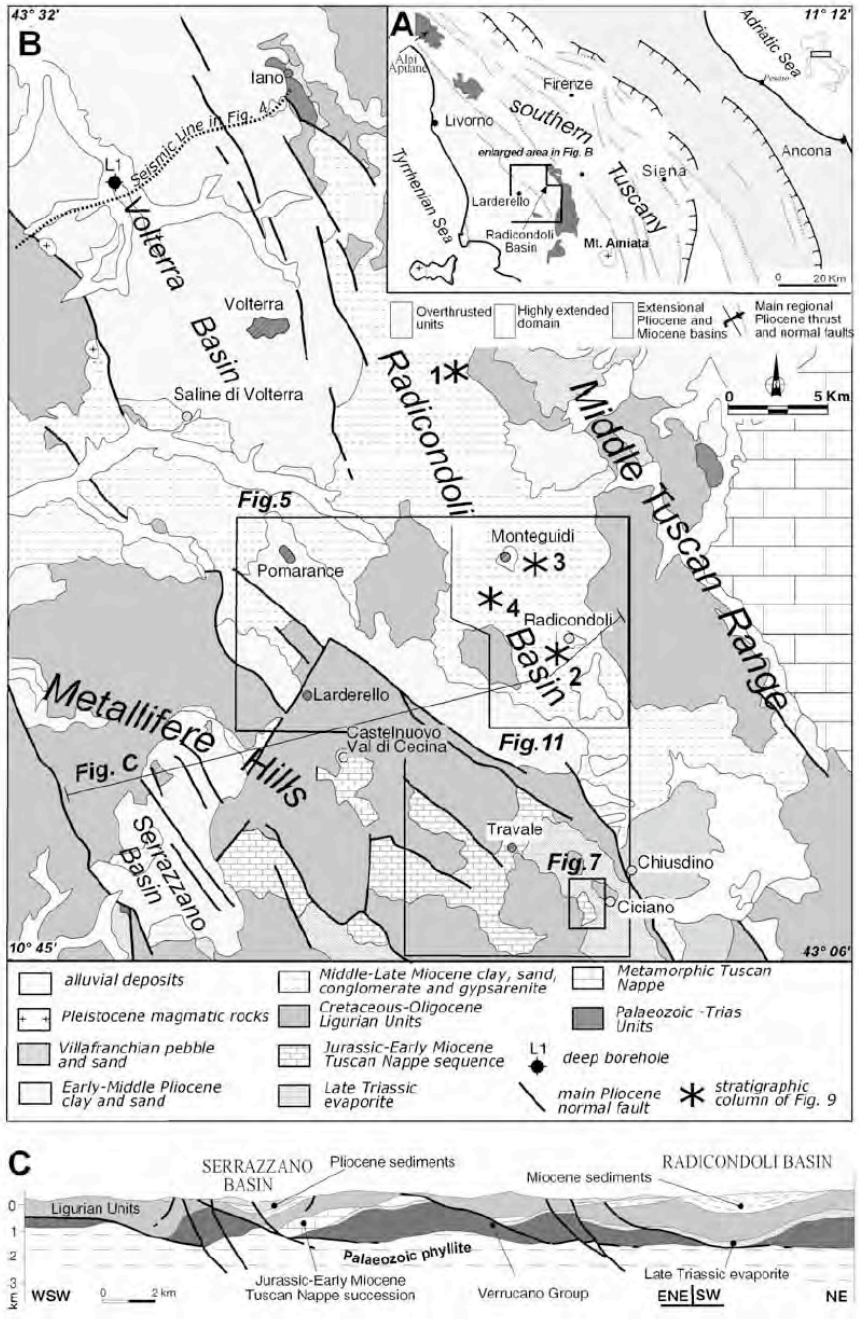

Figure 2

Brogi and Liotta 2004

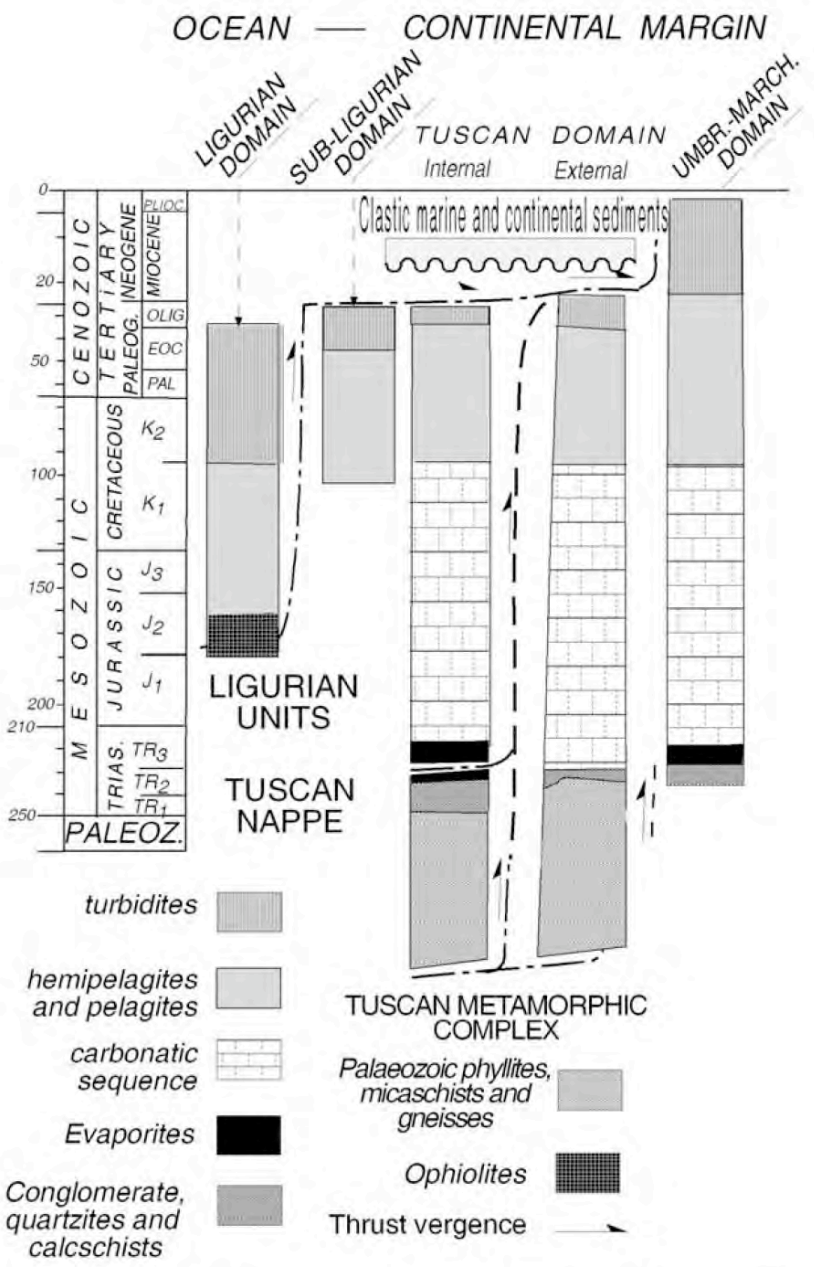

Figure 3. Relationships among the different tectonostratigraphic units of the inner northern Apennines and related paleogeographical domains (modified after *Carmignani et al.* [1994] with permission from Elsevier).

Brogi and Liotta 2004

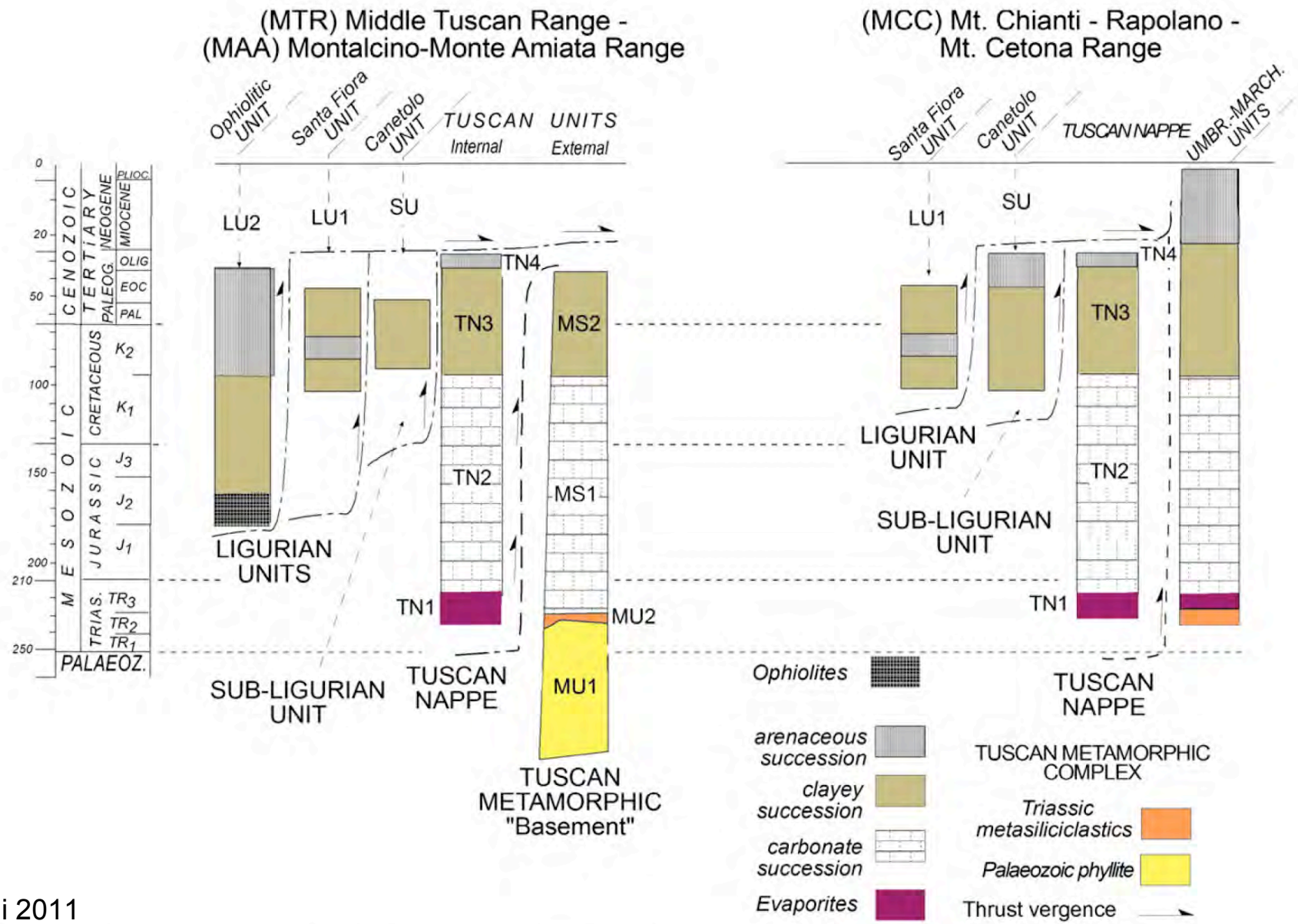

Brogi 2011

ig. 3. Relations among the different tectonic units of the Northern Apennines exposed in the indicated margins of the Siena basin. Symbols: LU — Ligurian Units: LU1 — Ophiolitic Unit; LU2 — S.Fiora Unit; SU — Subligurian Unit: Canetolo Unit; TN — Tuscan Nappe; TN1 — Late Triassic evaporites; TN2 — Late Triassic–Cretaceous carbonate and siliceous succession; TN3 — Late Cretaceous–Oligocene clayey (Scaglia Toscana) succession; TN4 — Oligocene–Early Miocene arenaceous (Macigno) succession; MU — Metamorphic Units: MU1 — Carboniferous–Permian phyllites and metasandstones; MU2 — Triassic metasiliciclastics; MS — Metamorphic Tuscan Nappe (Montagnola Senese Group): MS1 — Late Triassic–Cretaceous metacarbonate and metasiliceous succession; MS2 — Late Cretaceous–Eocene phyllite and matacarbonate succession.

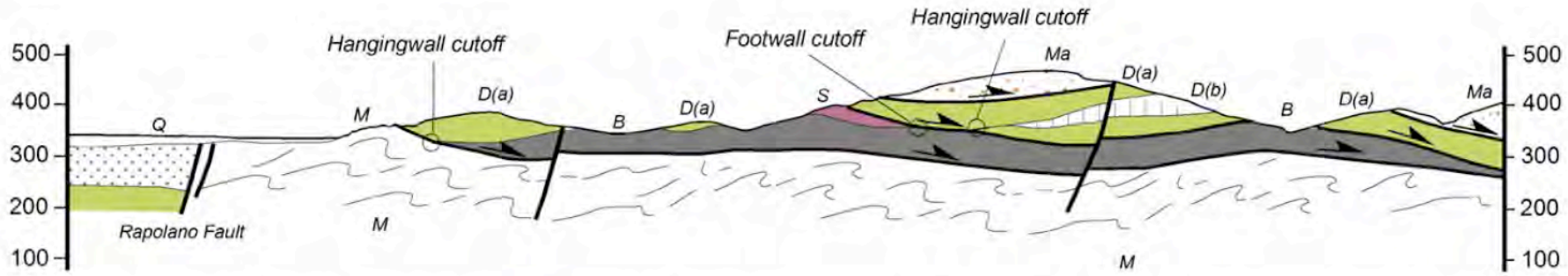

Fig. 5. Geological map of the Rapolano Terme area (see Fig. 2 for location) and related geological section. East-dipping low-angle normal faults gave rise to important tectonic omissions within the succession of the Tuscan Nappe. The low-angle normal faults were dissected by high-angle normal faults.

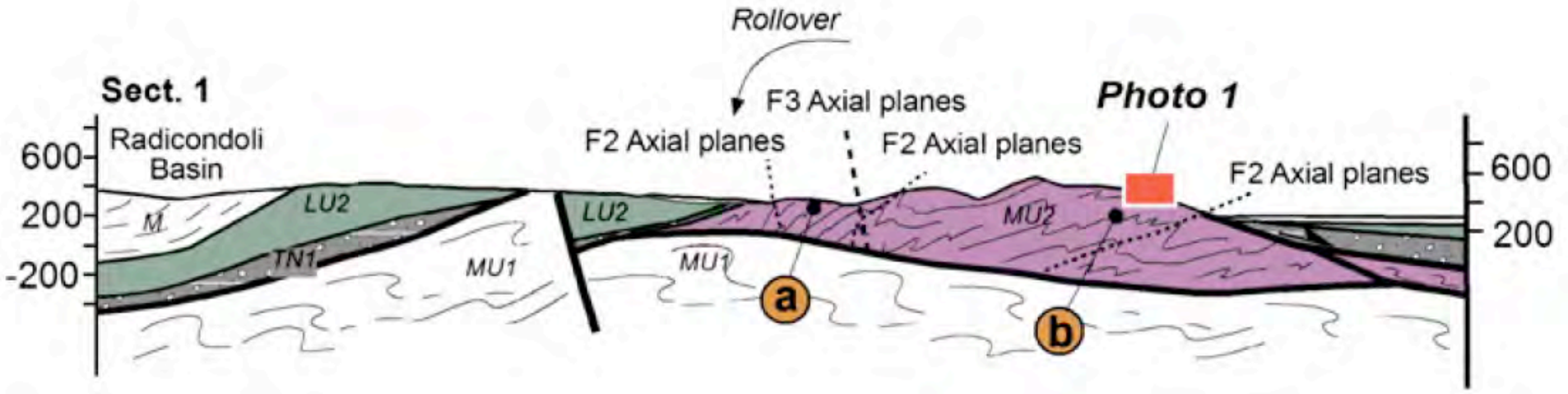

Brogi 2011

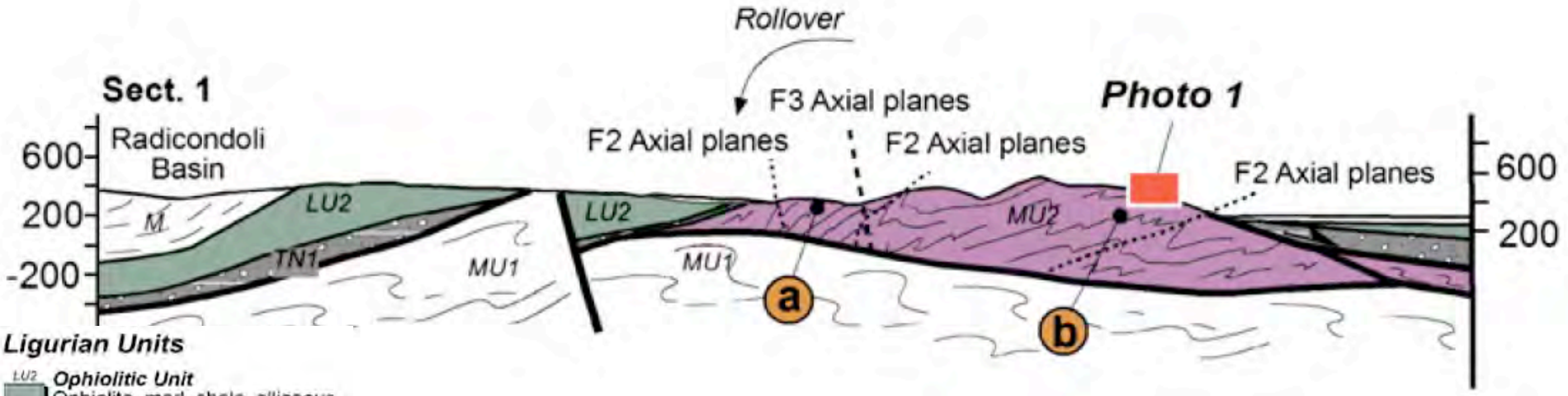

Ligurian Units

LU2 ***Ophiolitic Unit***
Ophiolite, marl, shale, siliceous limestone and radiolarite
Middle Jurassic-Early Cretaceous

LU1 ***S.Fiora Unit***
Marl, shale, sandstone limestone
Early Cretaceous - Eocene

Subligurian Unit

SU ***Canetolo Unit***
Calcarenite, marl, shale, limestones
Eocene

Tuscan Units

TN1 ***Tuscan Nappe***
Dolostone, gypsum, vacuolar limestone
Late Triassic

MU2 ***Metamorphic Units***
Metarenite, metapelite metaconglomerate
Triassic

MU1 Phyllite and metarenite
Paleozoic

Late Oligocene-Early Miocene thrust

Pliocene normal fault

Middle-Late Miocene low-angle normal fault

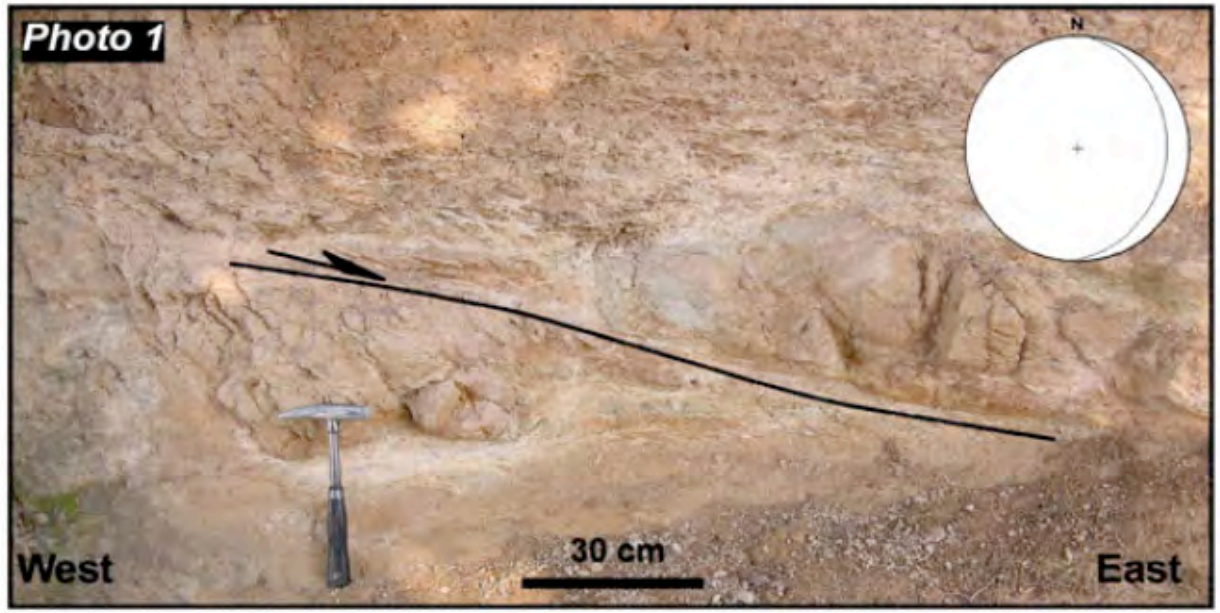

Brogi 2011

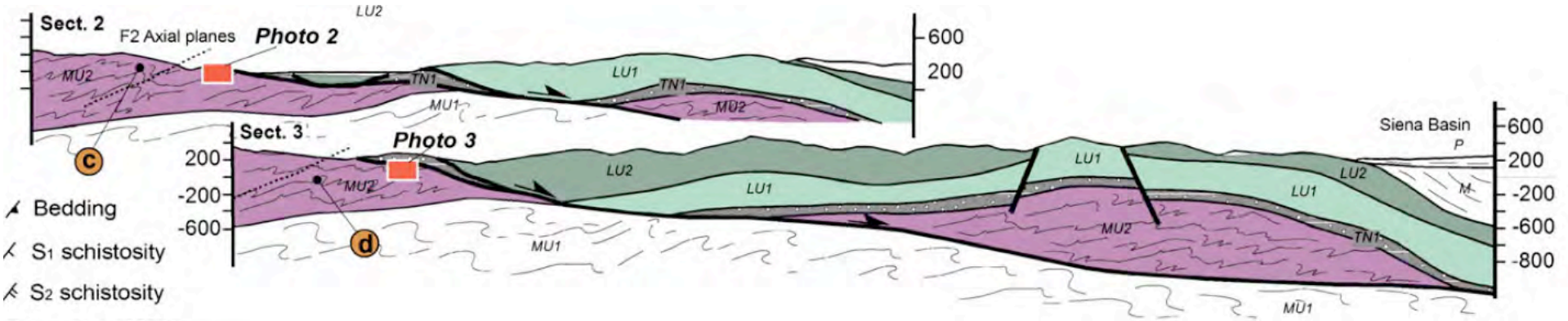

Ligurian Units

LU2 **Ophiolitic Unit**
Ophiolite, marl, shale, siliceous limestone and radiolarite
Middle Jurassic-Early Cretaceous

LU1 **S.Fiora Unit**
Marl, shale, sandstone limestone
Early Cretaceous - Eocene

Subligurian Unit

SU **Canetolo Unit**
Calcarenite, marl, shale, limestones
Eocene

Tuscan Units

TN1 **Tuscan Nappe**
Dolostone, gypsum, vacuolar limestone
Late Triassic

MU2 **Metamorphic Units**
Metarenite, metapelite metaconglomerate
Triassic

MU1 Phyllite and metarenite
Paleozoic

Late Oligocene-Early Miocene thrust

Pliocene normal fault

Middle-Late Miocene low-angle normal fault

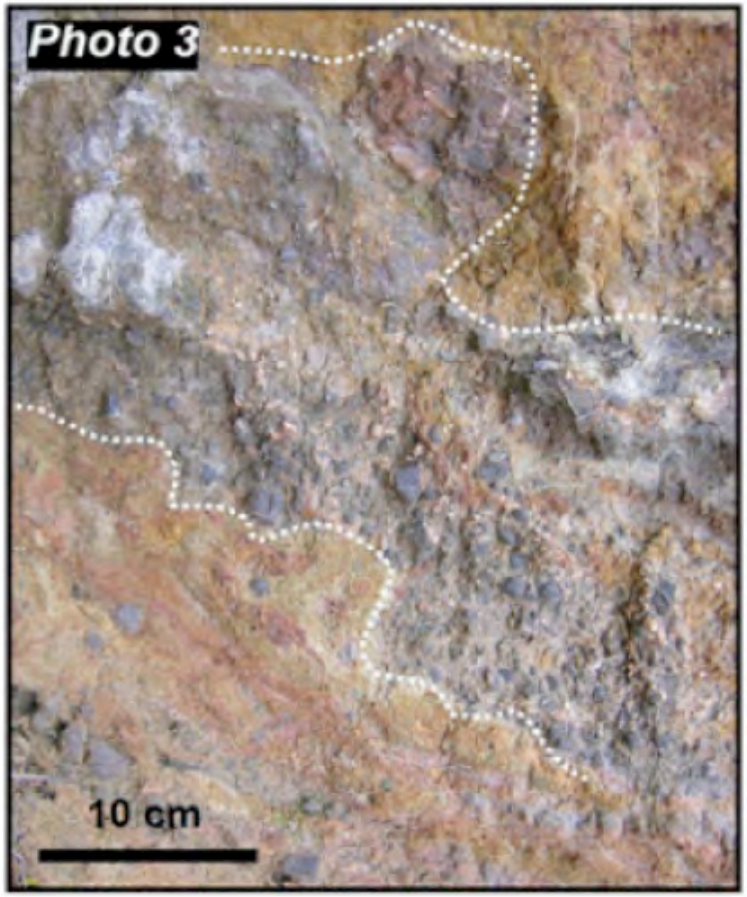

Brogi 2011

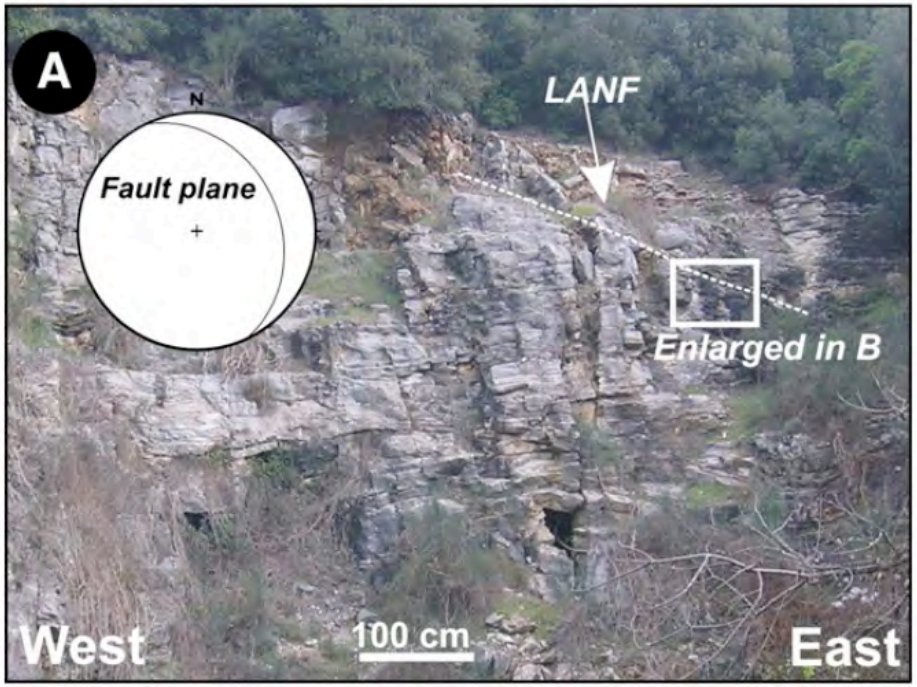

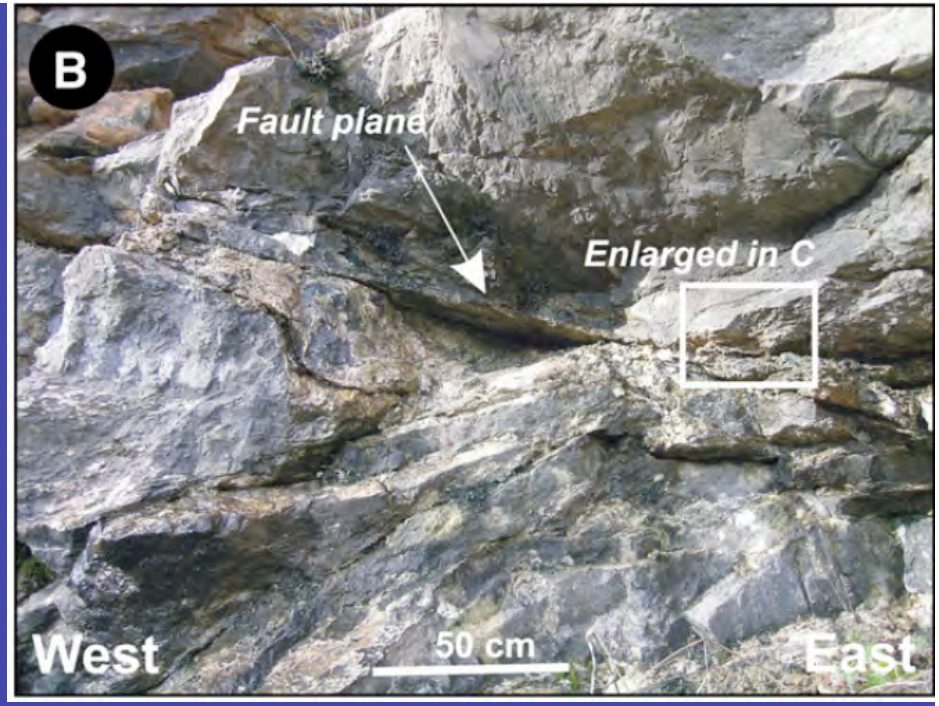

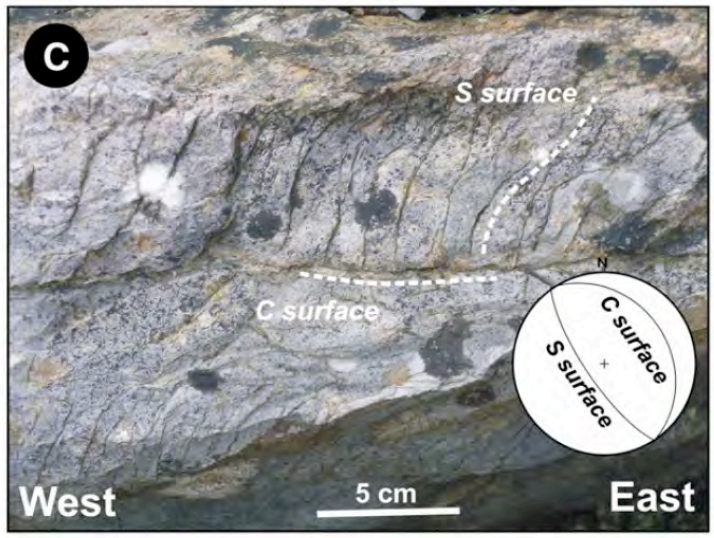

Fig. 7. Structures related to the extensional deformational events recognized in the Mt. Chianti–Rapolano–Mt. Cetona Range. See the text for more information. A) Low-angle normal faults affecting the Early Cretaceous limestones (Maiolica Fm) of the Tuscan Nappe. B) Particular of the fault plane and drag folds developed in the footwall. C) S–c structures in the hanging wall.

Brogi 2011

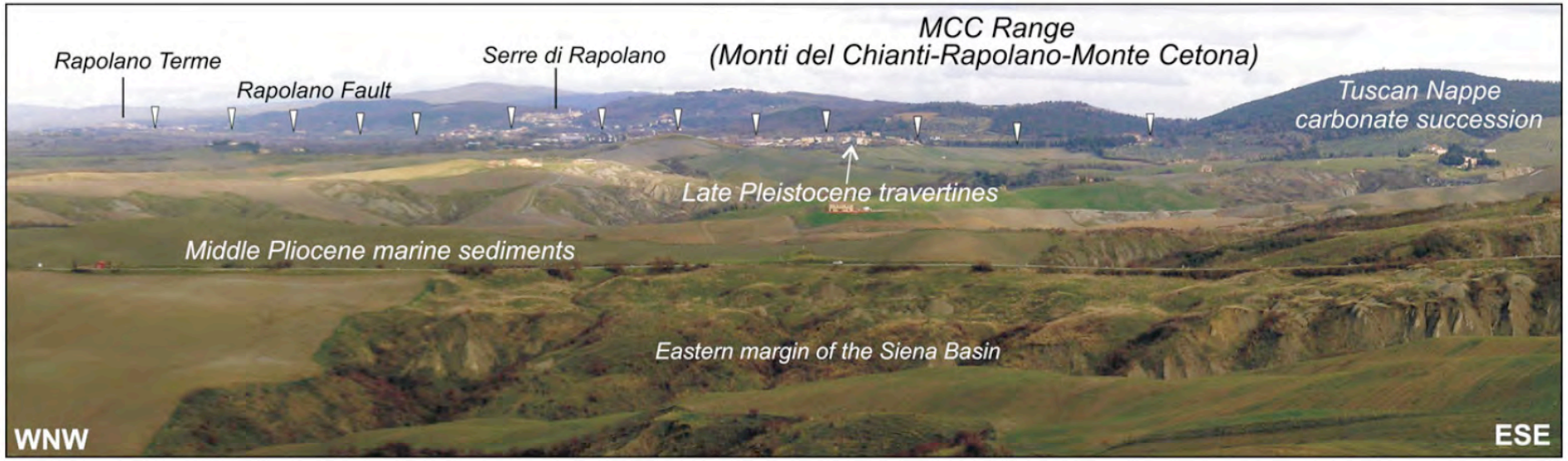

Fig. 8. Panoramic view of the Rapolano Fault trace indicated by the white triangles.

Brogi 2011

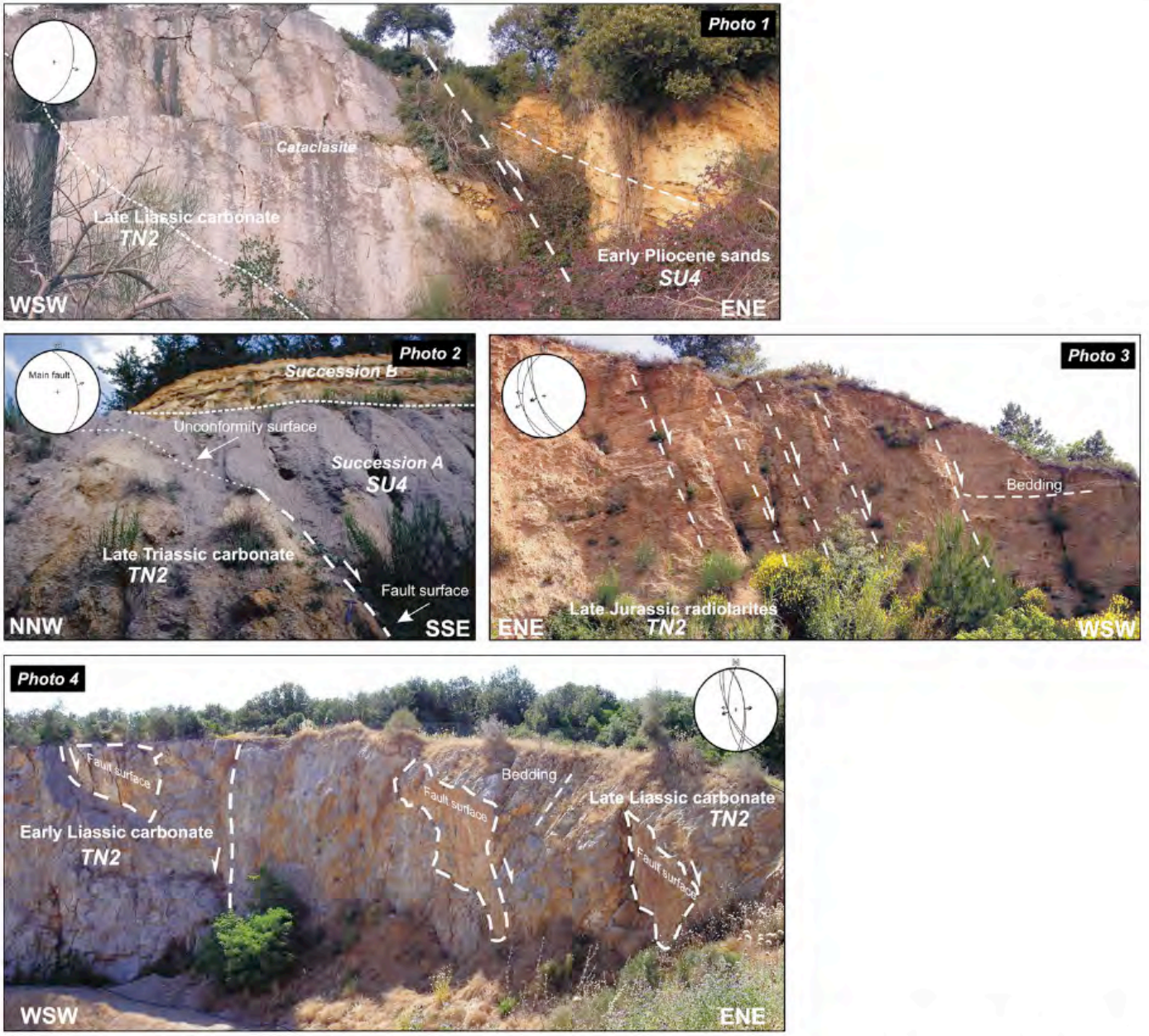

Fig. 10. Minor faults associated to the Rapolano Fault exposed in different outcrops indicated in the Fig. 9. Photo 1 illustrates a normal fault separating Early Pliocene sands and clayey-sands from the Late Jurassic carbonate (Calcare selcifero Fm) of the Tuscan Nappe. Photo 2 shows a sin-sedimentary normal faults active during the deposition of the succession A (Early–Middle Pliocene lignite bearing clay and silt); The Succession B (Middle Pliocene sands) buried the fault constraining its age (see the text for more information). Photo 3 illustrates parallel normal faults affecting Jurassic radiolarites (Diaspri Fm) of the Tuscan Nappe; Photo 4 shows some normal faults affecting Jurassic carbonates (Calcare massiccio Fm) of the Tuscan Nappe.

Brogi 2011

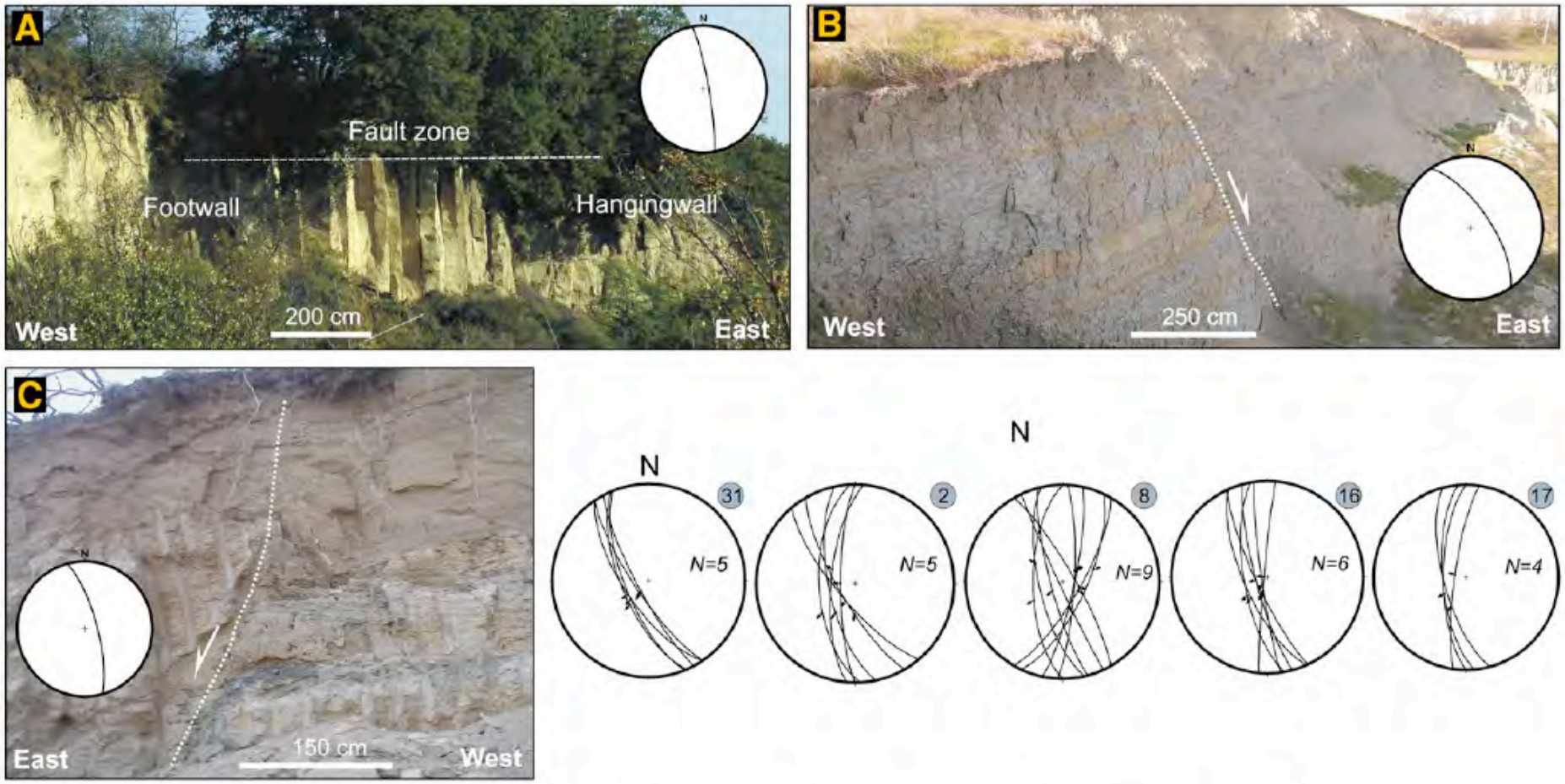

Fig. 12. Outcrop-scale normal and transtensional faults affecting the clayey succession forming the Stratigraphic Unit 4. The stereographic diagrams (Schmidt diagram, lower hemisphere) show faults and striae measured in the indicated structural stations: their locations are indicated in Fig. 2. A, B and C are described in the text.

Brogi 2011

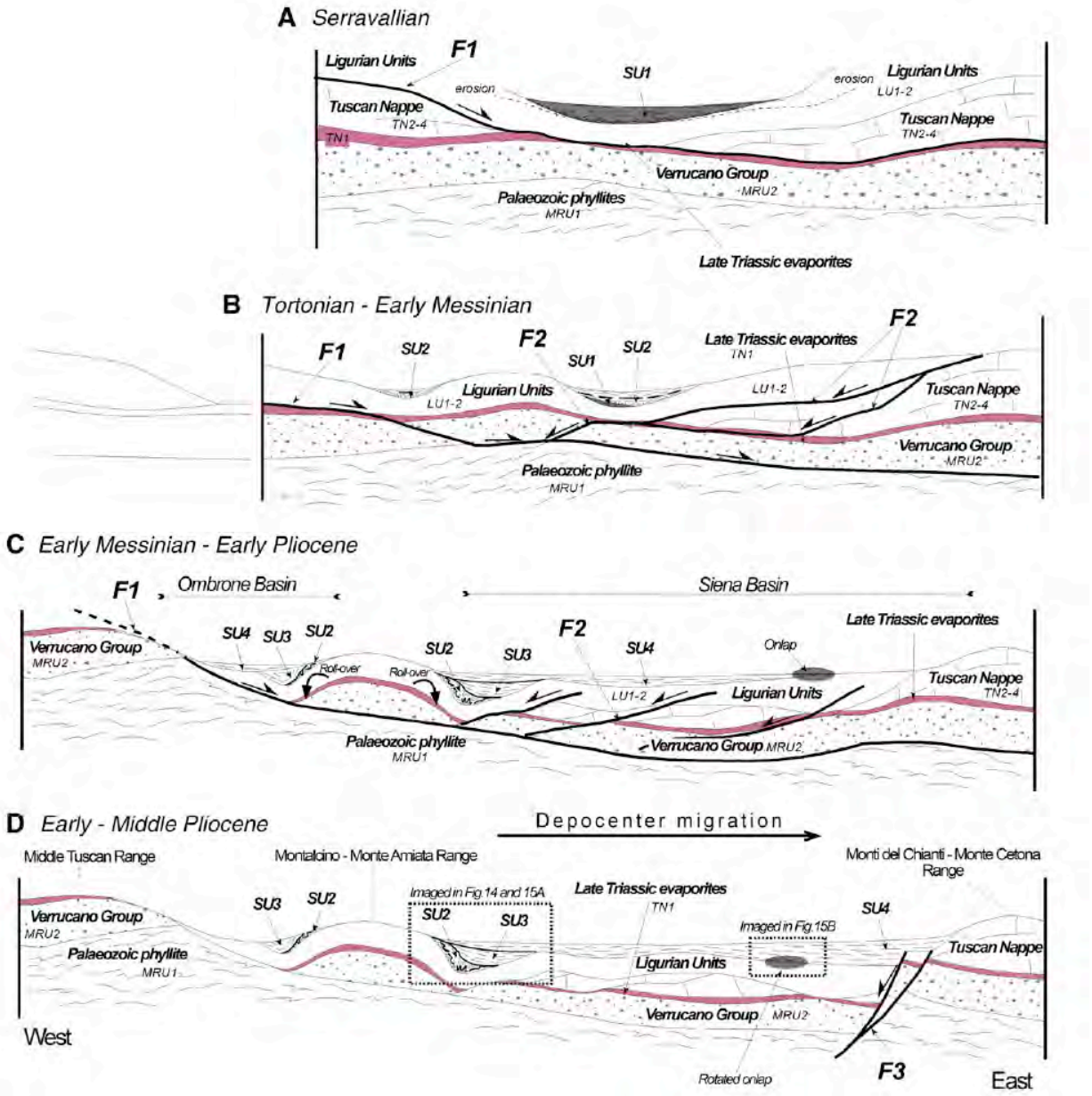

Fig. 18. Cartoon (not to scale) showing four stages illustrating the development of the Siena Basin. (A) The main east-dipping low-angle normal fault (F1) affected the stacked tectonic units after the collisional event; the main detachment level developed within the Late Triassic evaporite (TN1), producing the Tuscan Nappe lateral segmentation and a structural depression where the SU1 sediments deposited. B) Progressive faulting gave rise to the development of antithetic (west-dipping) low-angle normal faults (F2) contemporaneously with the deepening of the F1 fault accommodating at the top of the Palaeozoic phyllite (MRU1); the activity of the F2 faults produced the tectonic depression where the SU2 sediments deposited; C) the rotation of the hanging wall of the antithetic low-angle normal fault gave rise to the deformation of the SU2 deposits, and produced space accommodation for the SU3 sediments. SU4 sediments filled a broad structural depression and (D) were affected by west-dipping normal fault system (Rapolano Fault, F3) during Early–Pliocene times, mainly in the eastern side of the basin. Such a fault system dissected the previously developed low-angle normal faults.

Brogi 2011

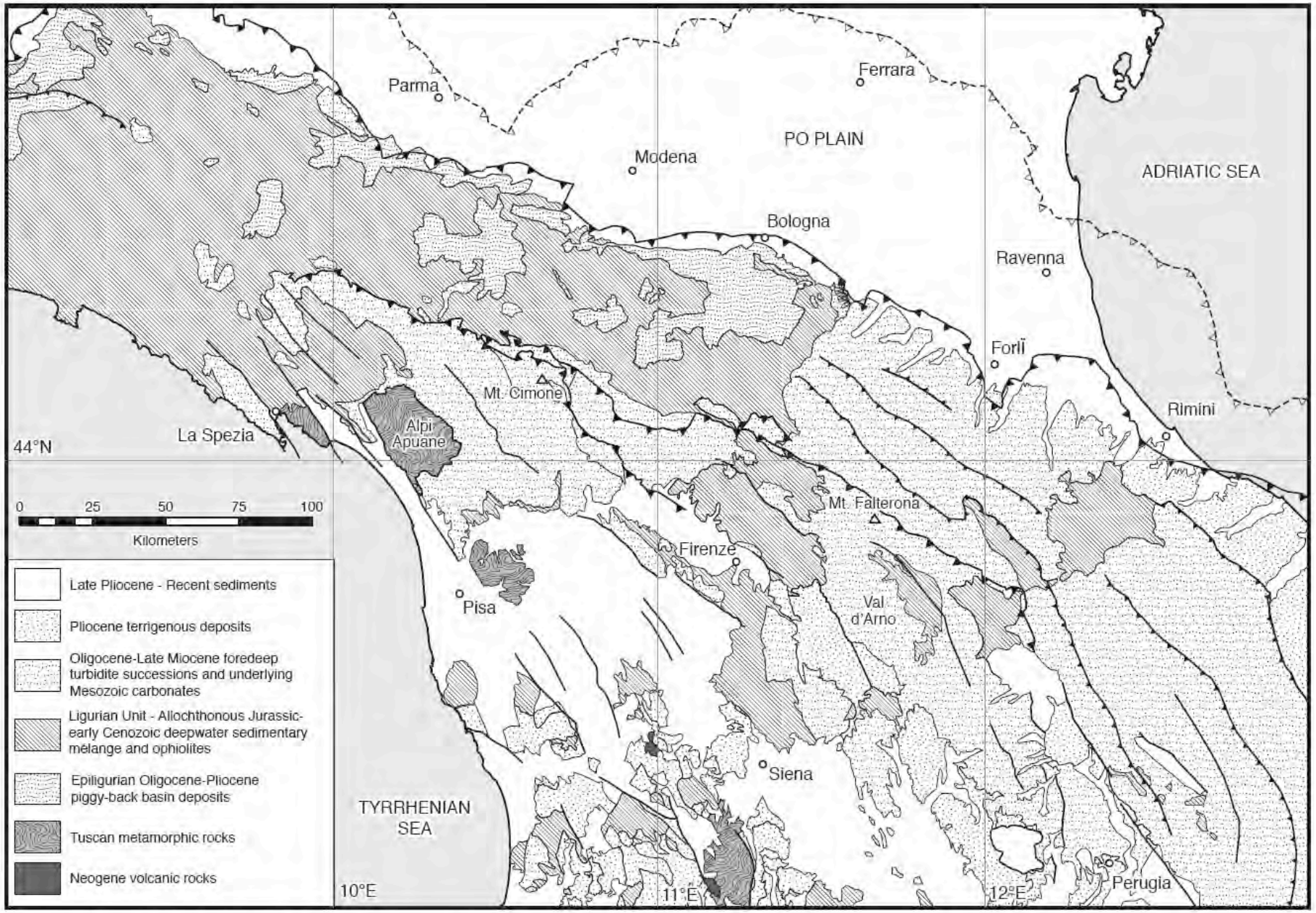

Thompson et al.

Figure 1. Geologic map of the northern Apennines, with location of the Mount Cimone, Mount Falterona, and Valdarno high-relief sample transects.

Thompson et al 2010

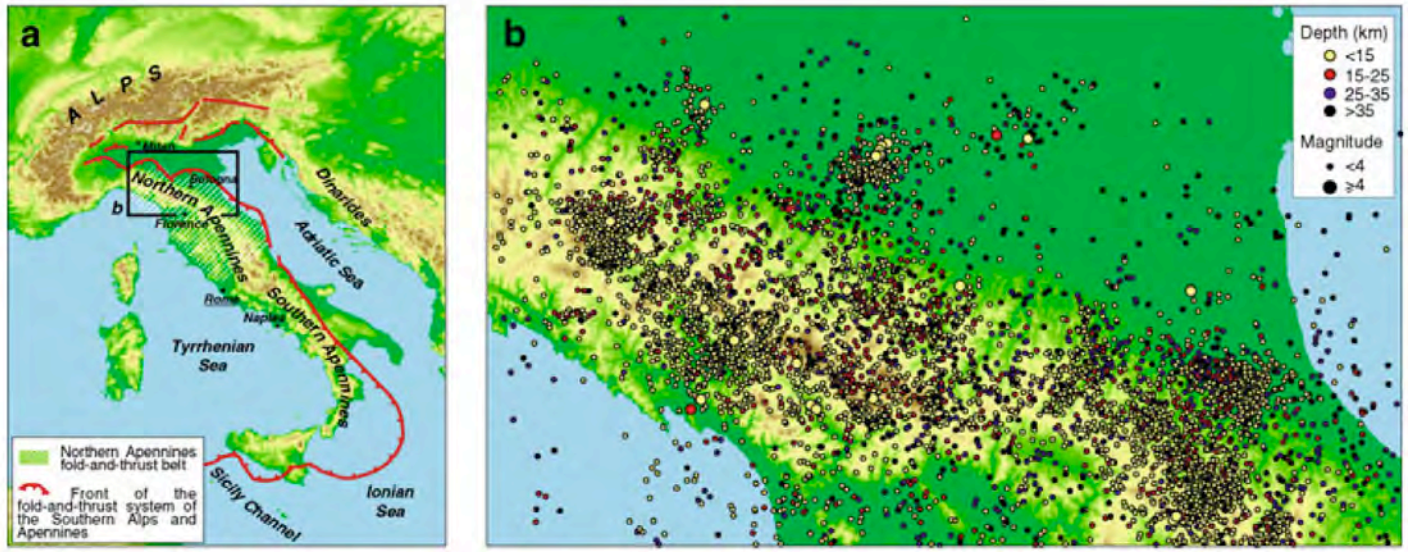

Fig. 1 **a** Schematic tectonic framework of Italy. **b** Seismicity of the Northern Apennines (after Boccaletti et al. 2004)

Boccaletti et al 2011

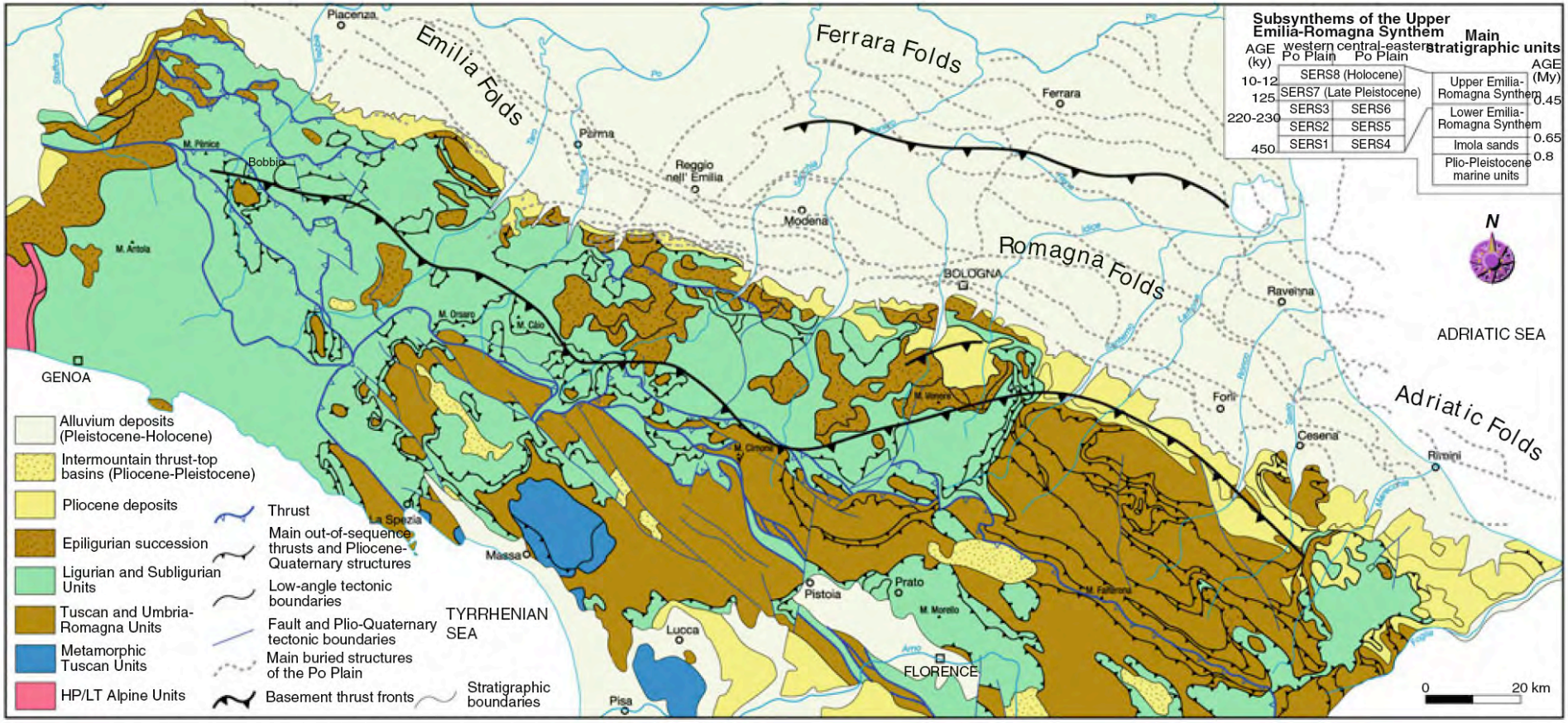

Fig. 2 Tectonic scheme of the Northern Apennines (after Pieri and Groppi 1981; Cerrina Feroni et al. 2002). *Inset on right upper corner* shows a stratigraphic scheme of the Neogene-Quaternary units of the Po Plain and the Apennnines–Po Plain margin

Boccaletti et al 2011

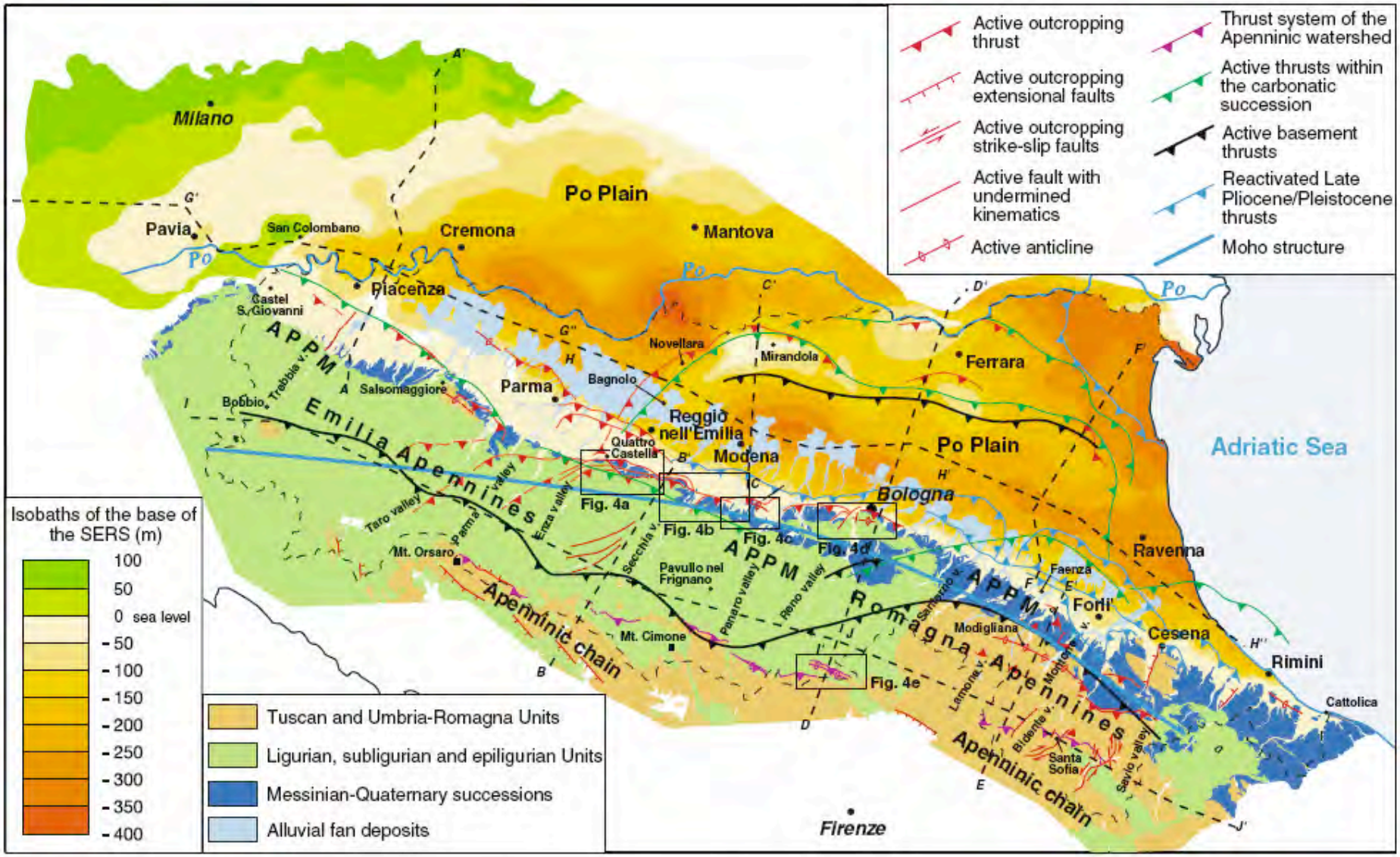

Fig. 3 Recent and active structures of the Emilia-Romagna. Subsurface geology in the Po Plain is illustrated as isobaths of the base of the Upper Emilia-Romagna Synthem (450,000 year). *APPM*: Apennines–Po Plain margin. *Solid lines with letters* indicate the trace of cross sections reported in Fig. 5

Boccaletti et al 2011

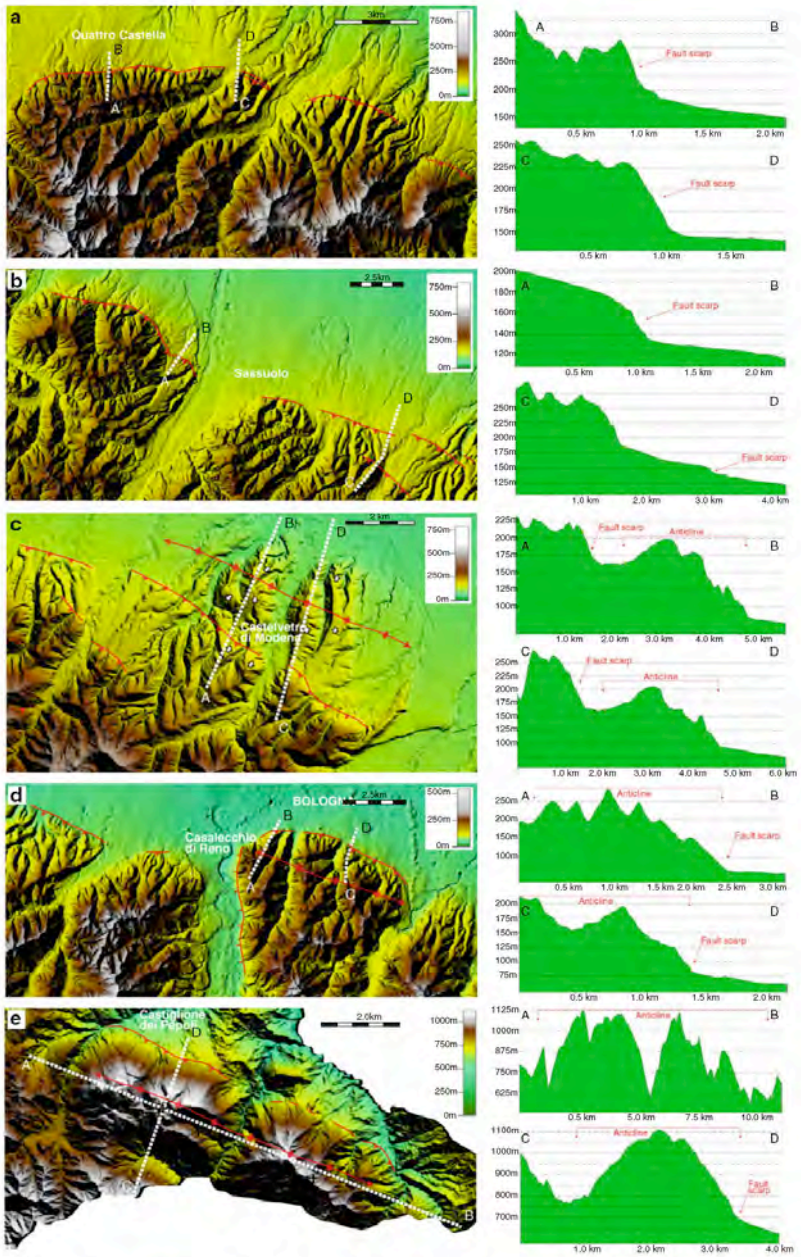

Fig. 4 Details of recent and active structures in the external part of the Northern Apennines illustrated as digital elevation models (DEMs) with 10-m resolution (*left panels*) and topographic profiles of the main structures (*right panels*). *Insets on left panels* represent a structural sketch of the main structures. **a** Pede-Apenninic Thrust Front near Quattro Castella. Note the prominent fault scarp associated with typical morphostructural features (such as triangular facets). **b** Pede-Apenninic Thrust Front near Sassuolo. **c** Pede-Apenninic Thrust Front and associated growing anticline in the Castelvetro di Modena area. *Arrows* indicate the tilting direction of paleo-surfaces. **d** Pede-Apenninic Thrust Front and associated growing anticline in the Bologna area. **e** Castiglione dei Pepoli thrust front and growing anticline. Location of different panels is reported in Fig. 3

Boccaletti et al 2011

Fig. 6 **a** Alluvial terraces (<220,000 year) in the S. Sofia area (Bidente valley); **b** tilted alluvial deposits (Lower Emilia-Romagna Synthem, 0.65–0.45 M year) (Tiepido valley, Modena Apennines–Po Plain margin); **c** overturned Imola Sands (0.8–0.65 M year) (Reno valley, Bologna Apennines–Po Plain margin); **d** Thrust faults affecting the Imola Sands (0.8–0.65 M year) (Panaro valley, Modena Apennines–Po Plain margin)

Boccaletti et al 2011

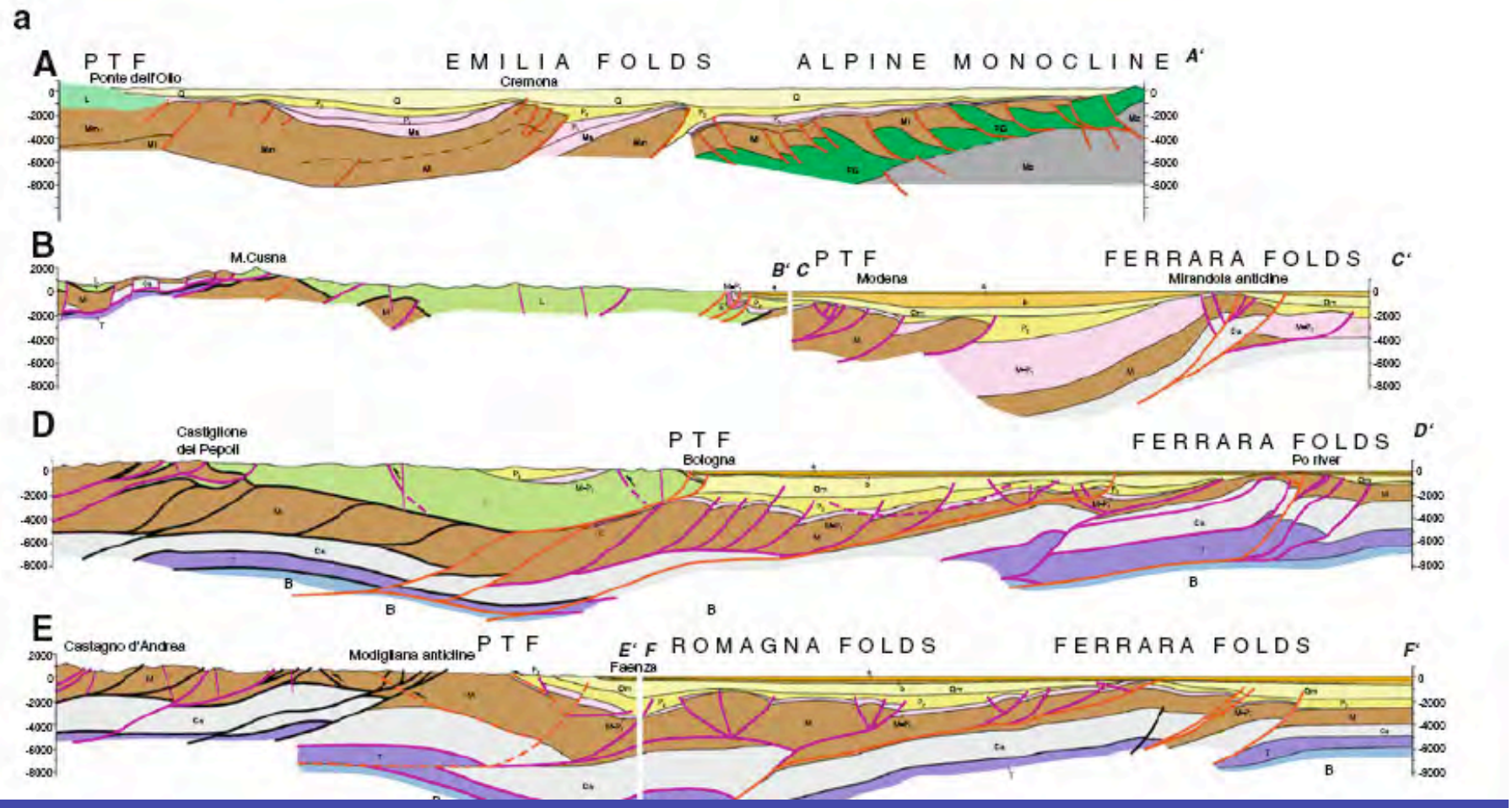

Fig. 5 Transversal (**a**) and longitudinal (**b–c**) geological cross sections of the external Northern Apennines. Location in Fig. 3. Modified from Pieri and Groppi (1981), Cassano et al. (1986), and Boccaletti et al. (2004). In the cross sections, unit a (Middle Pleistocene–Holocene) coincides with the Upper Emilia-Romagna Synthem and unit b (Middle Pleistocene) coincides with the Imola Sands + Lower Emilia-Romagna Synthem (see inset of Fig. 2). Note the occurrence of major thrust systems affecting the basement (*B*) close to Castiglione dei Pepoli (section *D–D′*) and Modigliana (section *E–E′*)

Boccaletti et al 2011

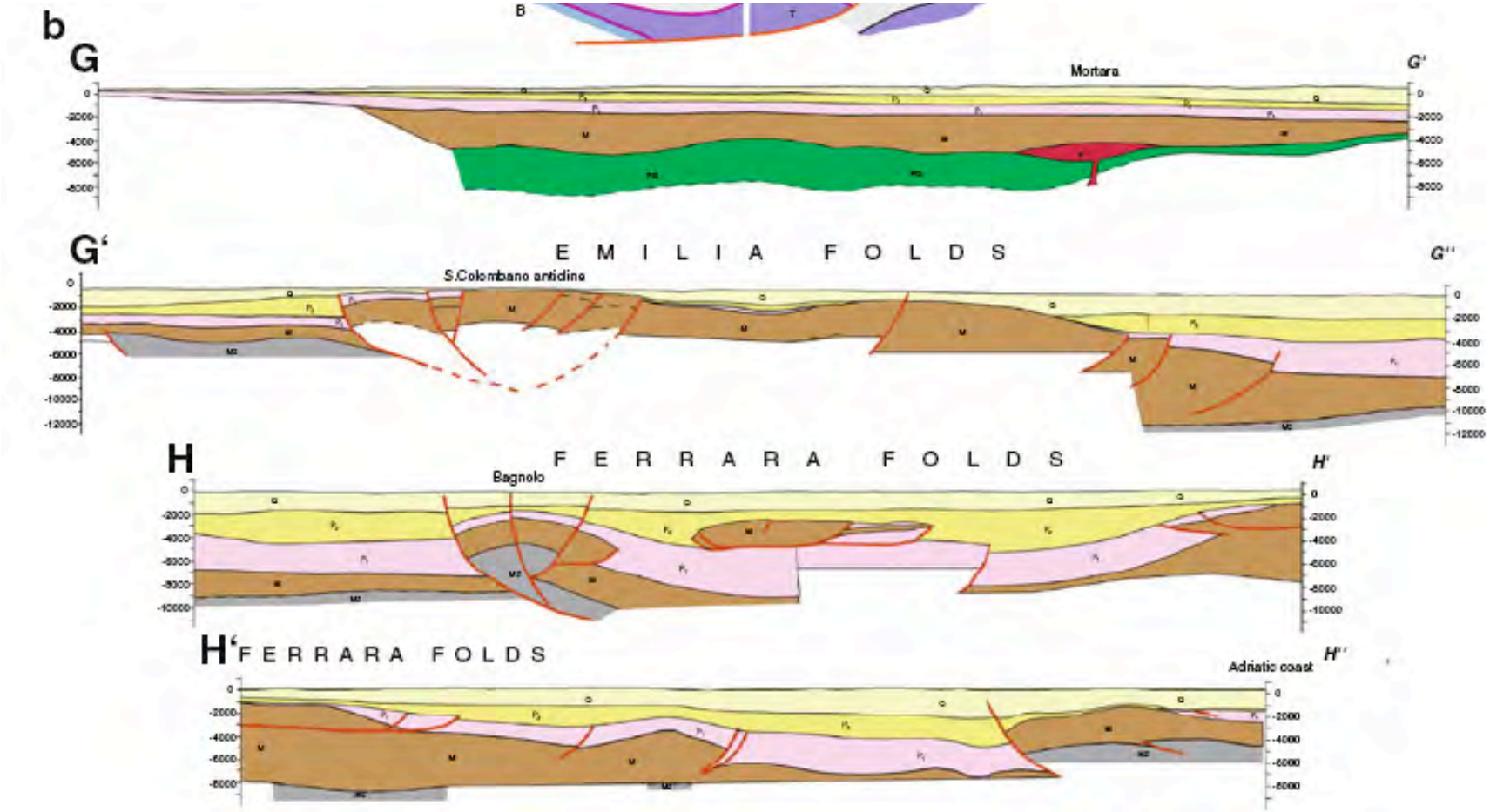

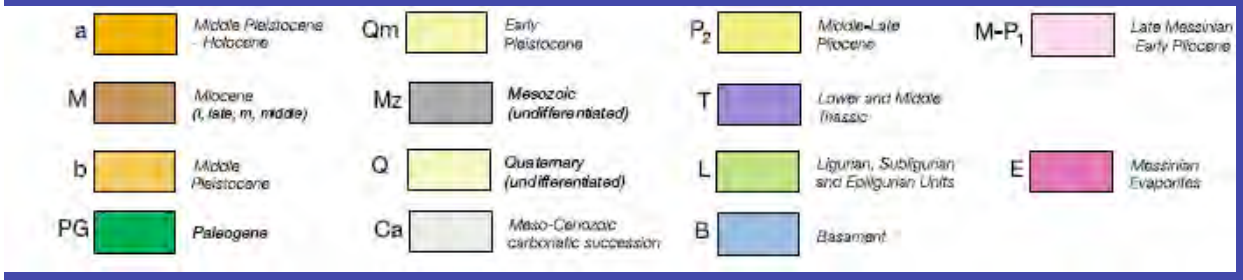

Fig. 5 Transversal (**a**) and longitudinal (**b–c**) geological cross sections of the external Northern Apennines. Location in Fig. 3. Modified from Pieri and Groppi (1981), Cassano et al. (1986), and Boccaletti et al. (2004). In the cross sections, unit a (Middle Pleistocene–Holocene) coincides with the Upper Emilia-Romagna Synthem and unit b (Middle Pleistocene) coincides with the Imola Sands + Lower Emilia-Romagna Synthem (see inset of Fig. 2). Note the occurrence of major thrust systems affecting the basement (*B*) close to Castiglione dei Pepoli (section *D–D′*) and Modigliana (section *E–E′*)

Boccaletti et al 2011

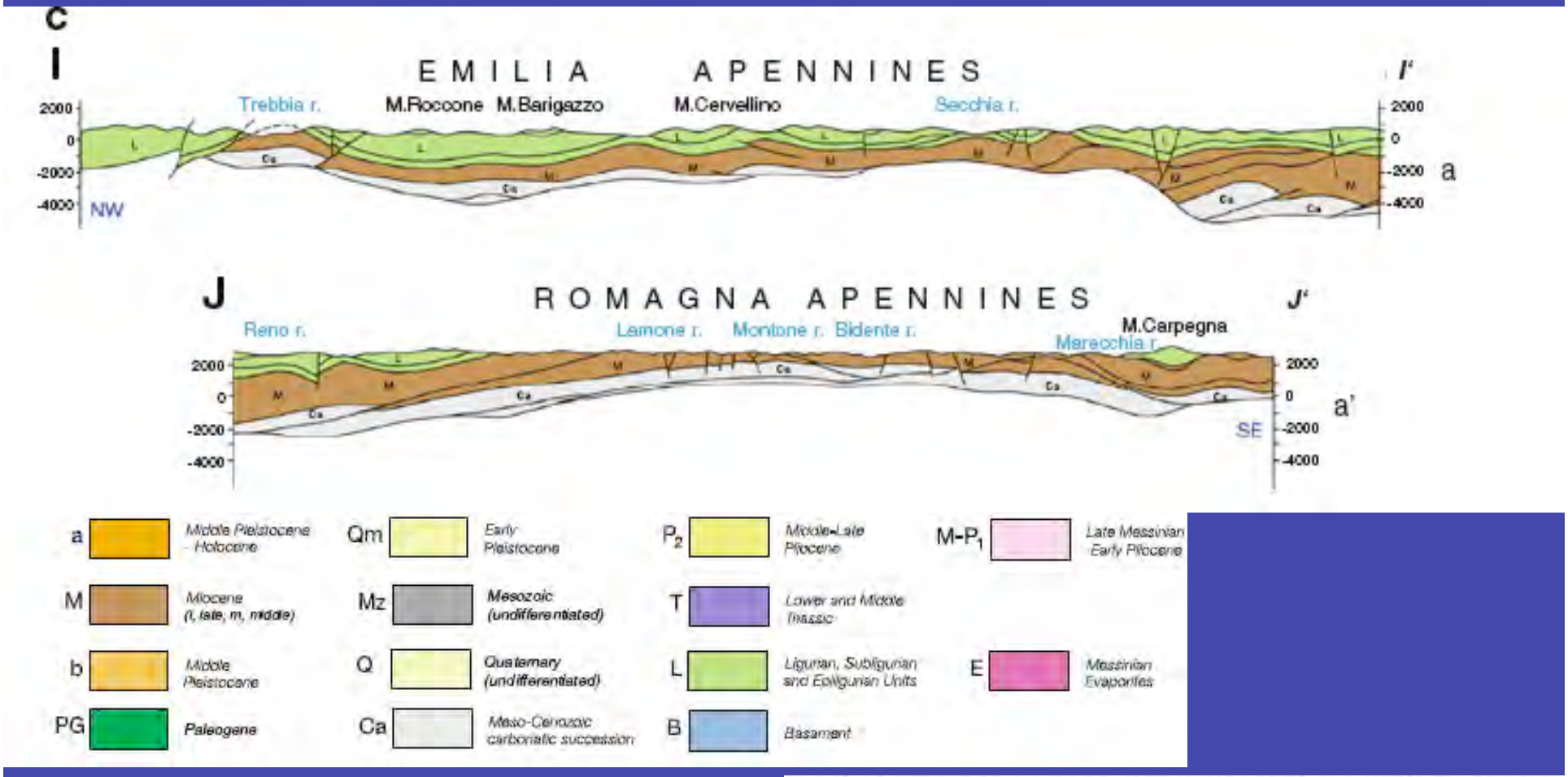

Fig. 5 Transversal (**a**) and longitudinal (**b–c**) geological cross sections of the external Northern Apennines. Location in Fig. 3. Modified from Pieri and Groppi (1981), Cassano et al. (1986), and Boccaletti et al. (2004). In the cross sections, unit a (Middle Pleistocene–Holocene) coincides with the Upper Emilia-Romagna Synthem and unit b (Middle Pleistocene) coincides with the Imola Sands + Lower Emilia-Romagna Synthem (see inset of Fig. 2). Note the occurrence of major thrust systems affecting the basement (*B*) close to Castiglione dei Pepoli (section *D–D′*) and Modigliana (section *E–E′*)

Boccaletti et al 2011

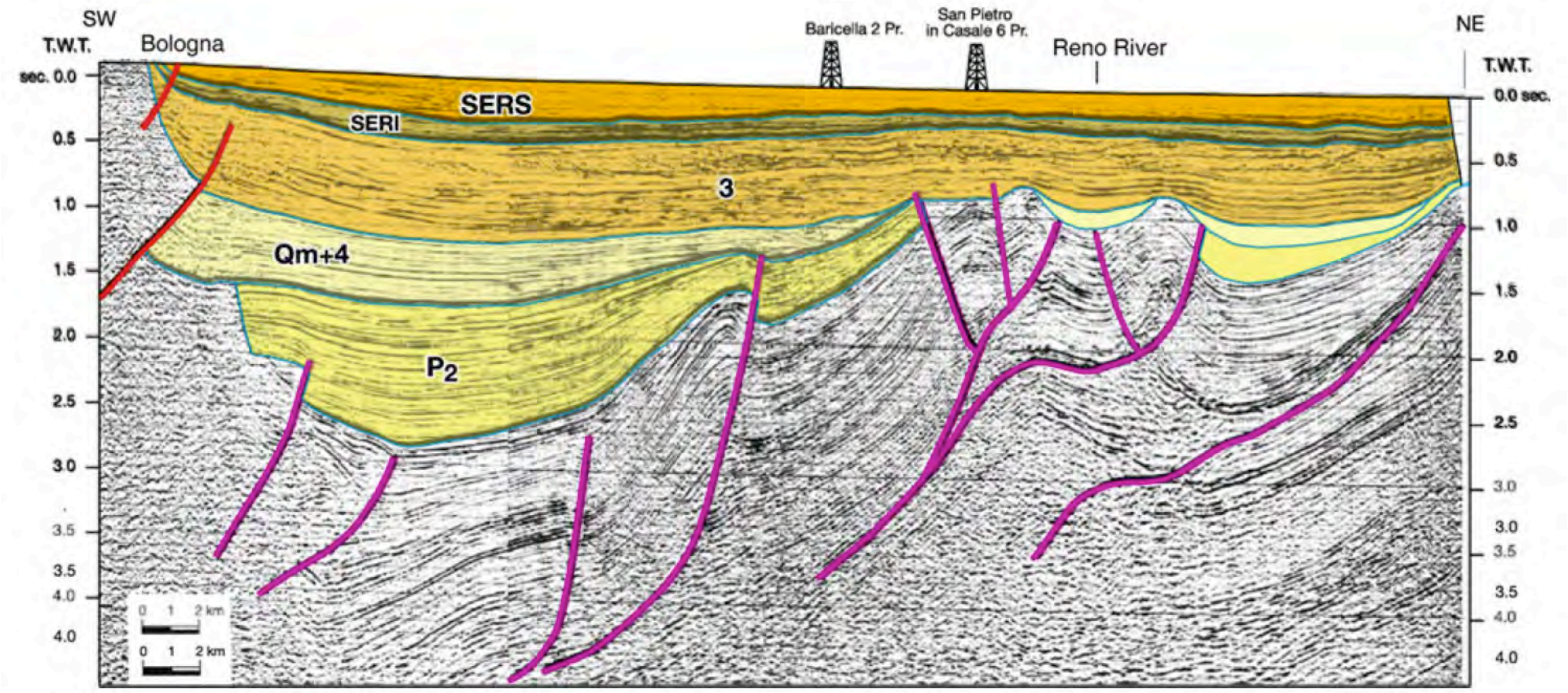

Fig. 7 Example of interpreted seismic line (modified from RER and ENI-Agip 1998). Note that Middle Pleistocene and Late Pleistocene units (*3*: Imola Sands; *SERI*: Lower Emilia-Romagna Synthem; *SERS*: Upper Emilia-Romagna Synthem) are folded and faulted. *P2*: Late Pliocene; *Qm*: Lower Pleistocene marine sediments; *4*: Yellow Sands (1–0.8 M year)

Boccaletti et al 2011

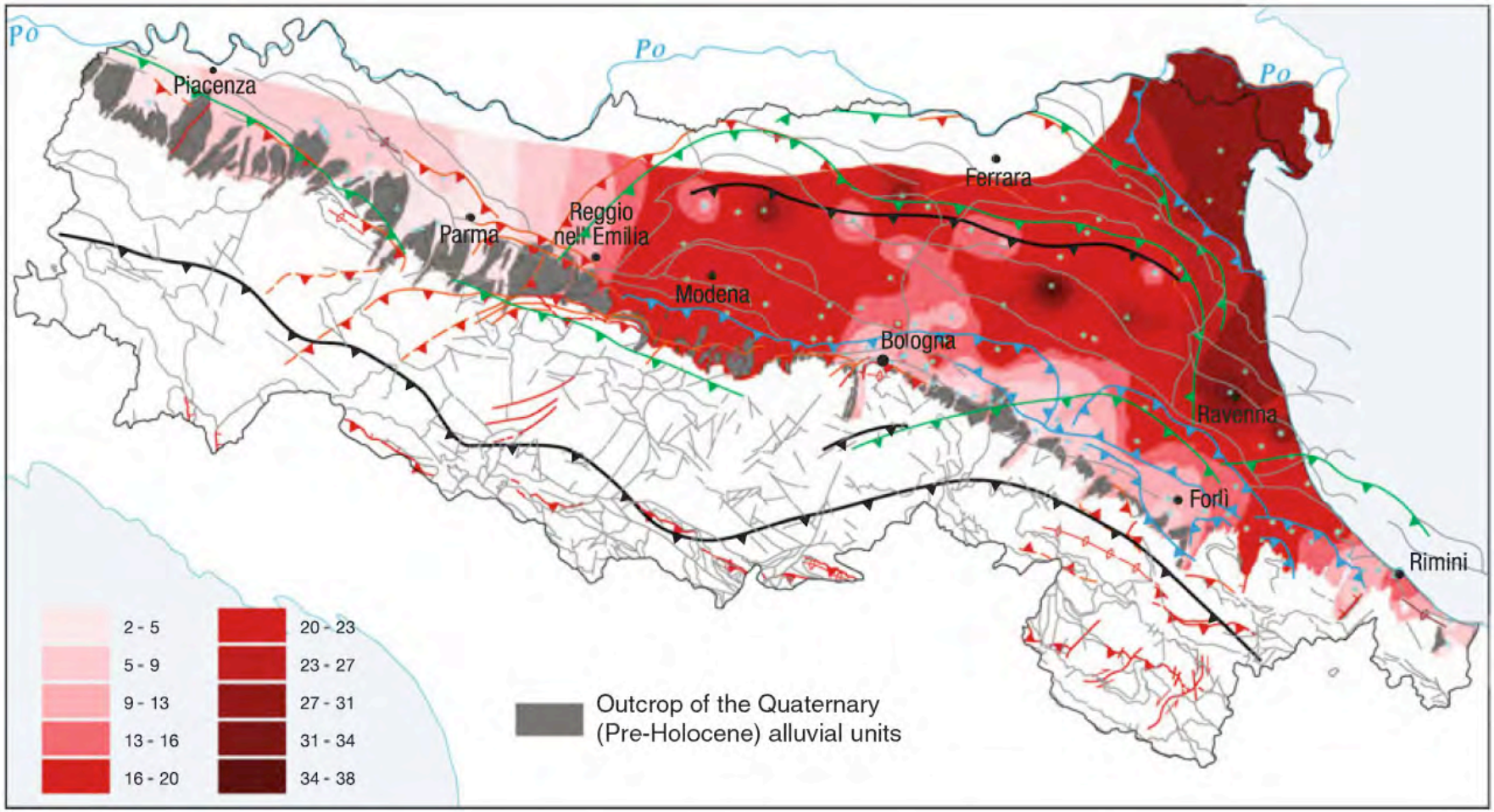

Fig. 8 Depth of the base of the Holocene (map legend indicates depths in metres from the surface)

Boccaletti et al 2011

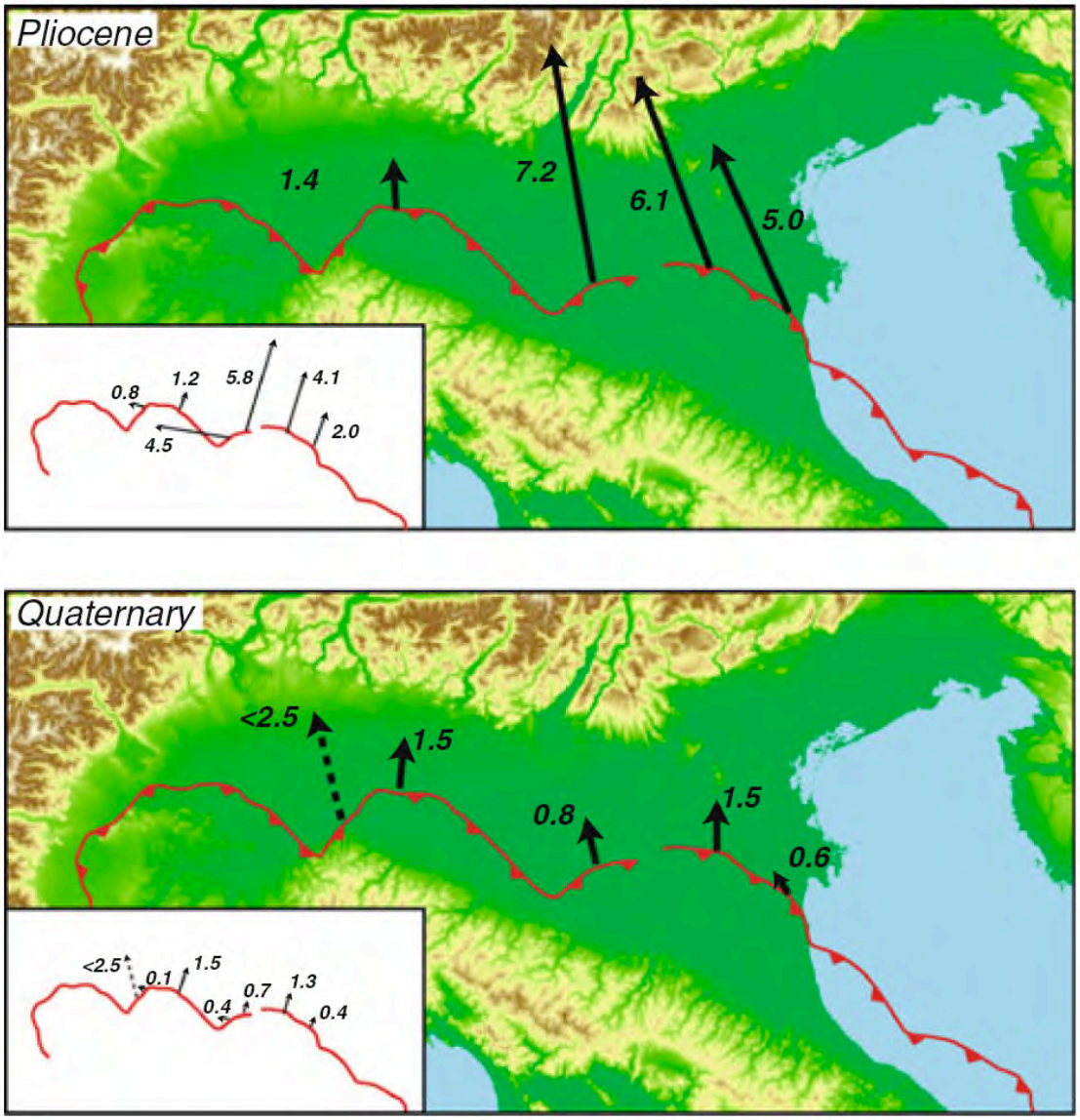

Fig. 10 Pliocene and Quaternary slip rates calculated from the main structures from analysis of available seismic sections. *Inset* shows rates along WNW–ESE and NNE–SSW seismic lines used to calculate the real shortening directions (see "Appendix" for details of calculations)

Boccaletti et al 2011

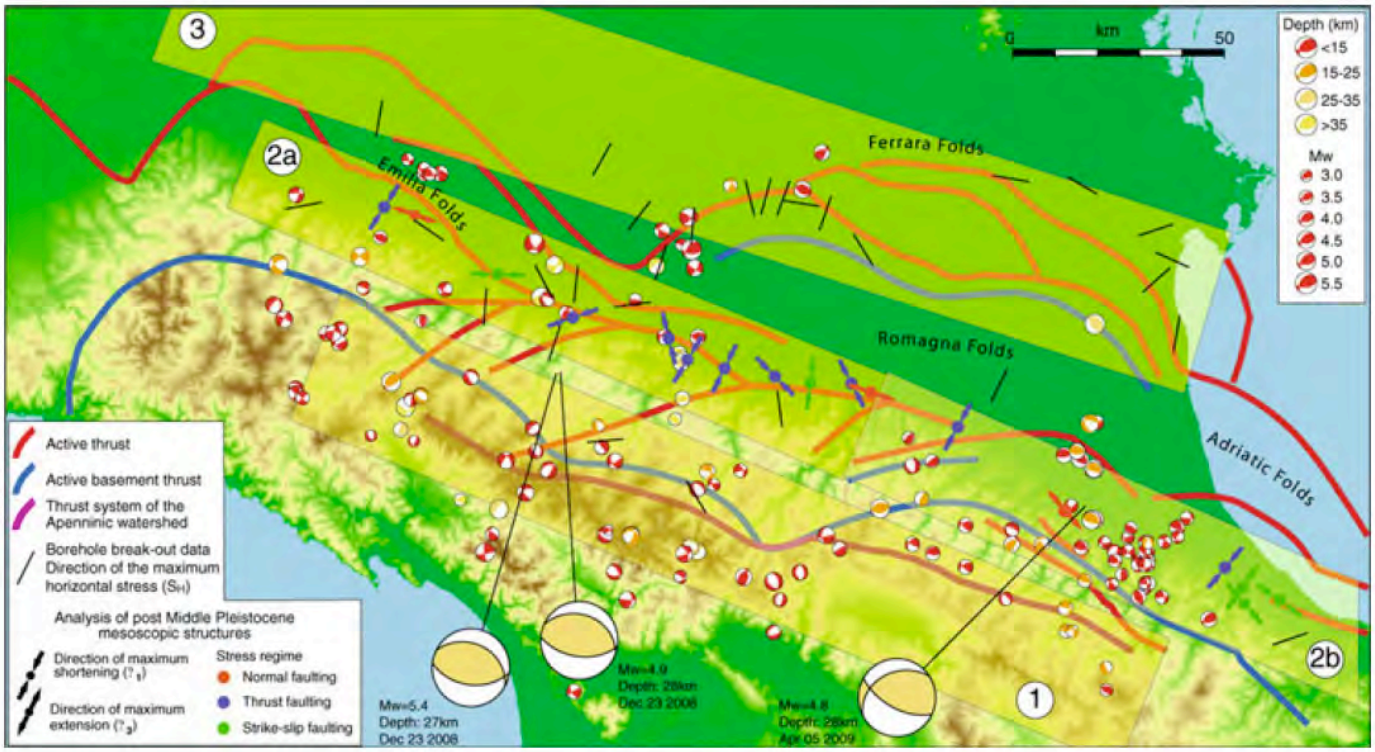

Fig. 11 Summary of the recent and active structures of the external Northern Apennines with superimposed focal mechanism solutions (Boccaletti et al. 2004), stress fields from mesoscopic analysis (Ghiselli and Martelli 1997) and borehole breakout data (Mariucci and Muller 2003). Enlarged are three focal mechanisms of main events of the seismic sequences that effected the external Apennines on December 23, 2008, and April 5, 2009 (from INGV data, http://www.ingv.it). *Numbers in circles* indicate the main fault systems: (*1*) Apenninic chain; (*2a*) Apennines–Po Plain margin (North-Western sector); (*2b*) Apennines–Po Plain margin (South-Eastern sector); (*3*) buried Emilia and Ferrara Folds

Boccaletti et al 2011

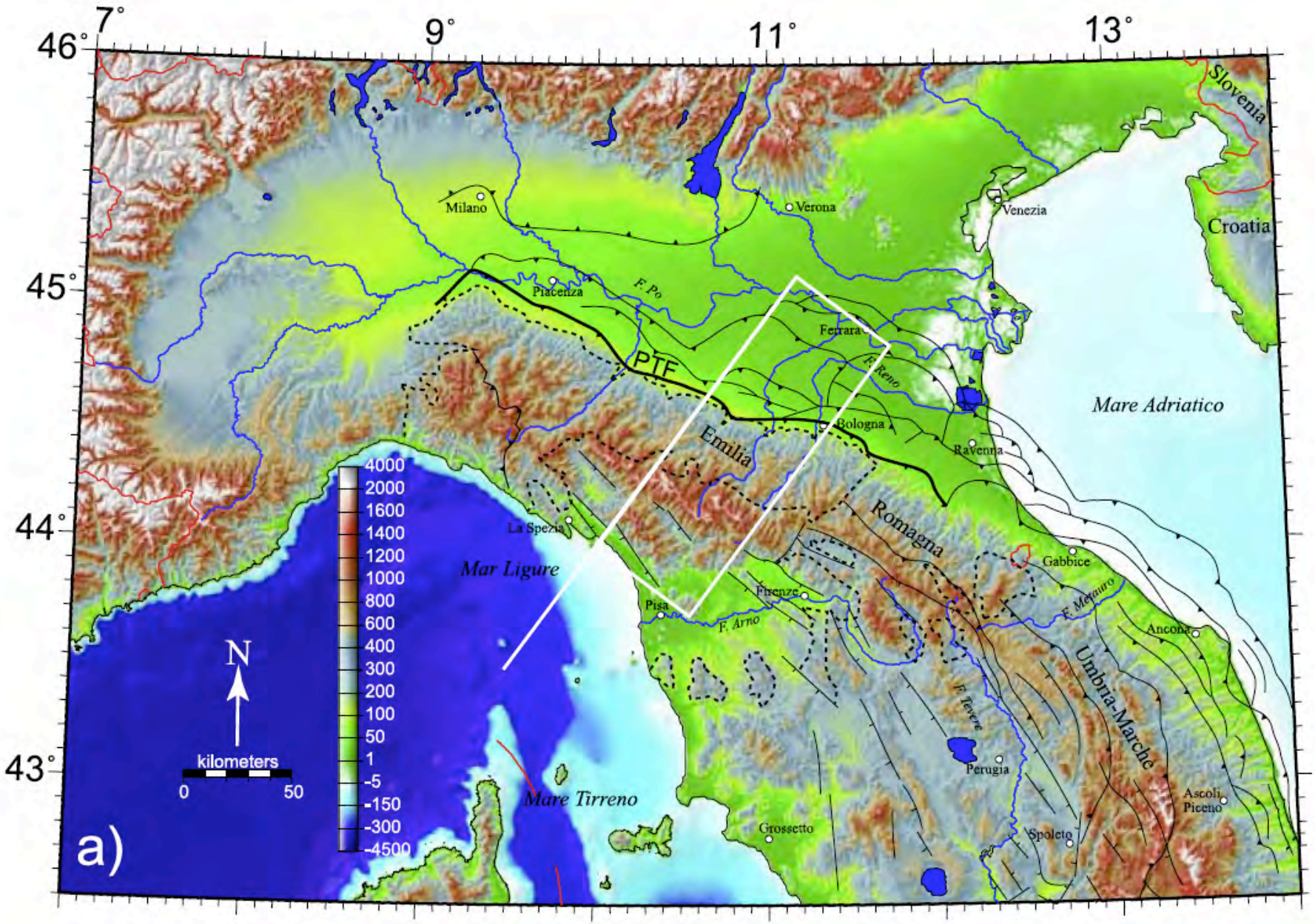

Picotti and Pazzaglia 2008

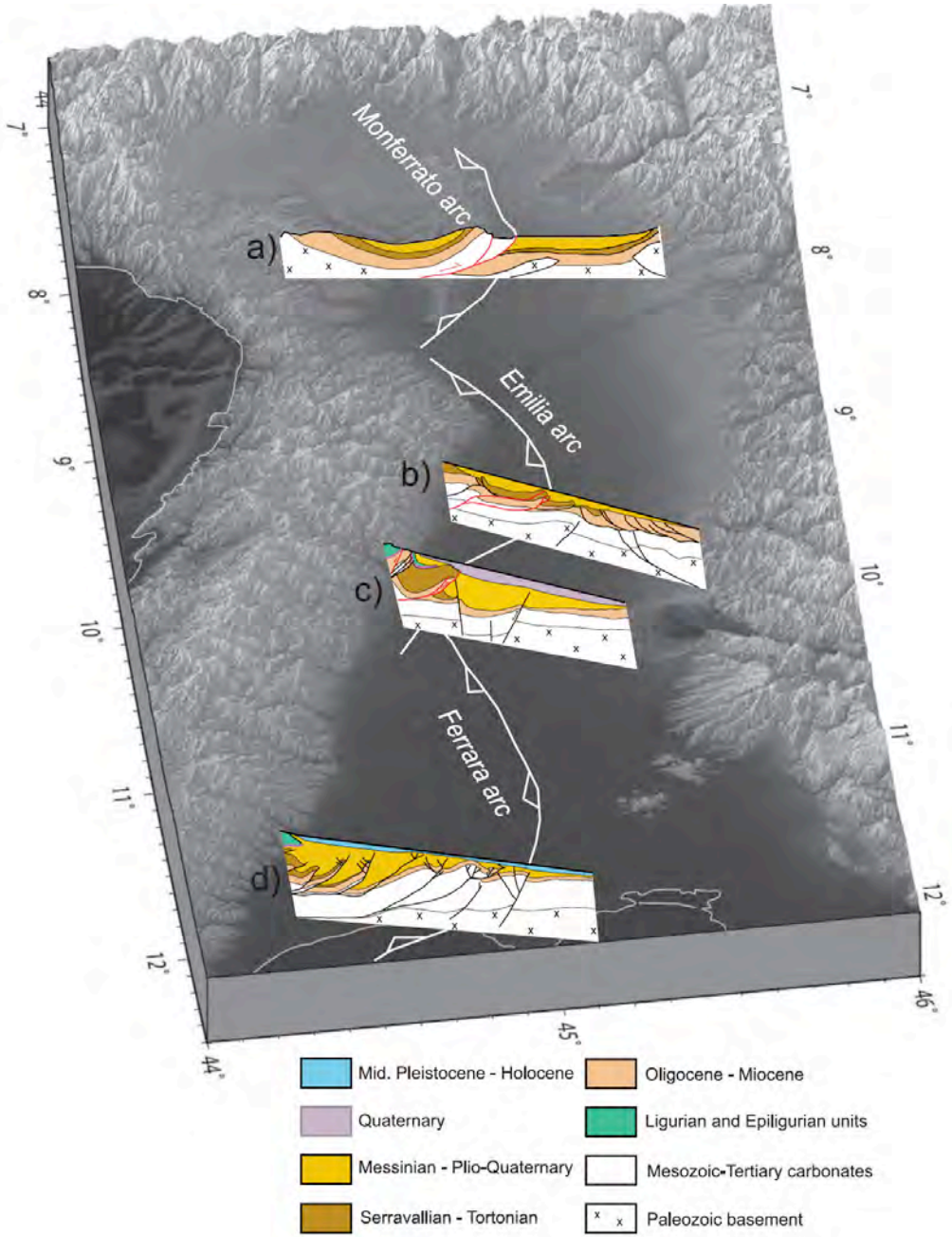

Figure 3. The geometry of the Po Plain basins. Transition from the Messinian-Plio-Quaternary wedge-shaped basin to the Pleistocene-Holocene sag basin (dotted patterns) began in the west (up on the figure) and progressed to the east (down on the figure). (a) From *Bertotti et al.* [2006]; (b) from *Bello and Fantoni* [2002]; (c) from *Picotti et al.* [2007]; (d) our data (see Figure 8).

Picotti and Pazzaglia 2008

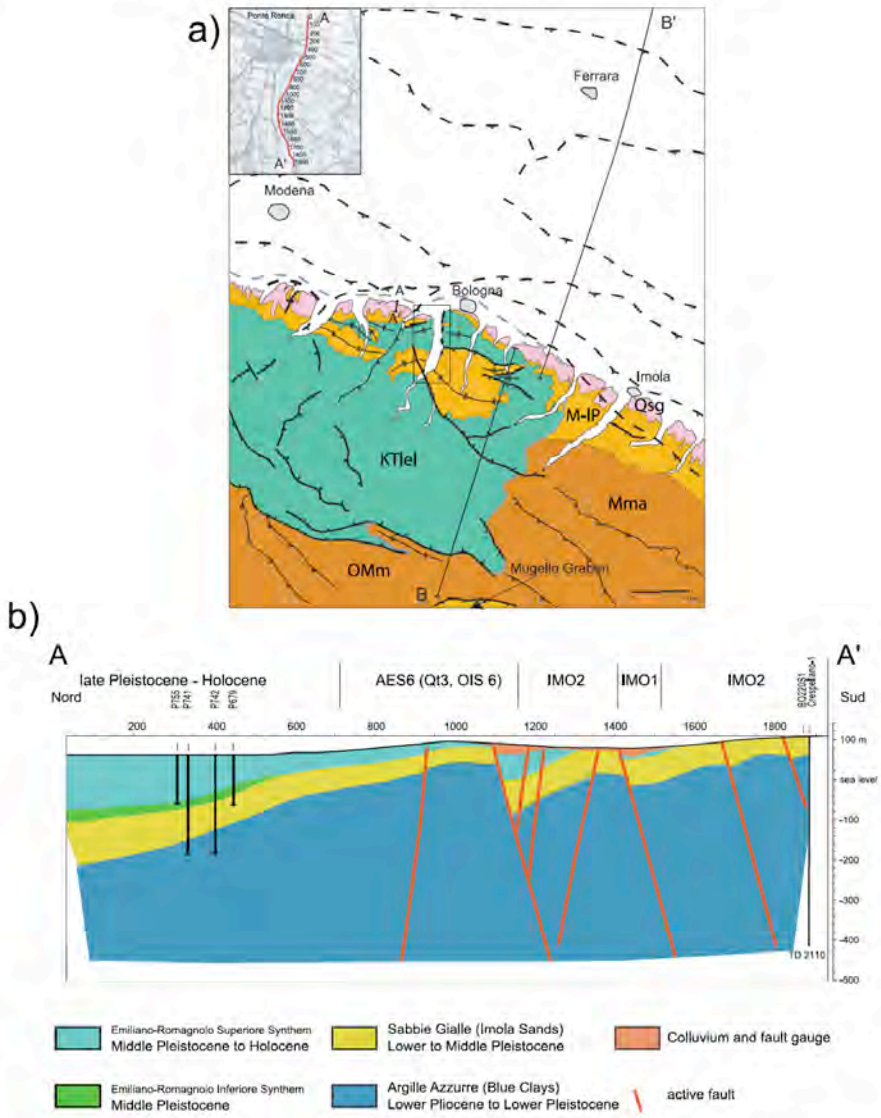

Figure 4. (a) Structural sketch of the northern Apennines around Bologna, with track of the cross-sections of Figure 4b (A–A′) and Figure 8 (B–B′). (b) Preliminary geologic interpretation of the Ponte Ronca seismic line from a preliminary coarse depth migration (not shown) and scaled for no vertical exaggeration. The stratigraphic nomenclature above the interpretation is from the 1:10,000 scale maps of Servizio Geologico Emilia-Romagna and *Martelli et al.* [2008] and defined in Table 1. Note the local mismatch between surface geology and line interpretation. Vertical lines between stratigraphic units indicate contacts on the 1:10,000 scale geologic map. Well logs are on file with the Servizio Geologico Emilia-Romagna and are courtesy of Paolo Severi. The box indicates the extent of the mapped area in Figure 5. Qsg, Sabbie Gialle (IMO1 and IMO2); M-lP, Miocene and lower Pliocene marine sediments including Pliocene Argille Azzure; Mma, Miocene Marnoso-arenacea; OMm, Oligocene-Miocene Macigno Fm.; KTlel, Cretaceous and Tertiary Ligurian and epi-Ligurian rocks.

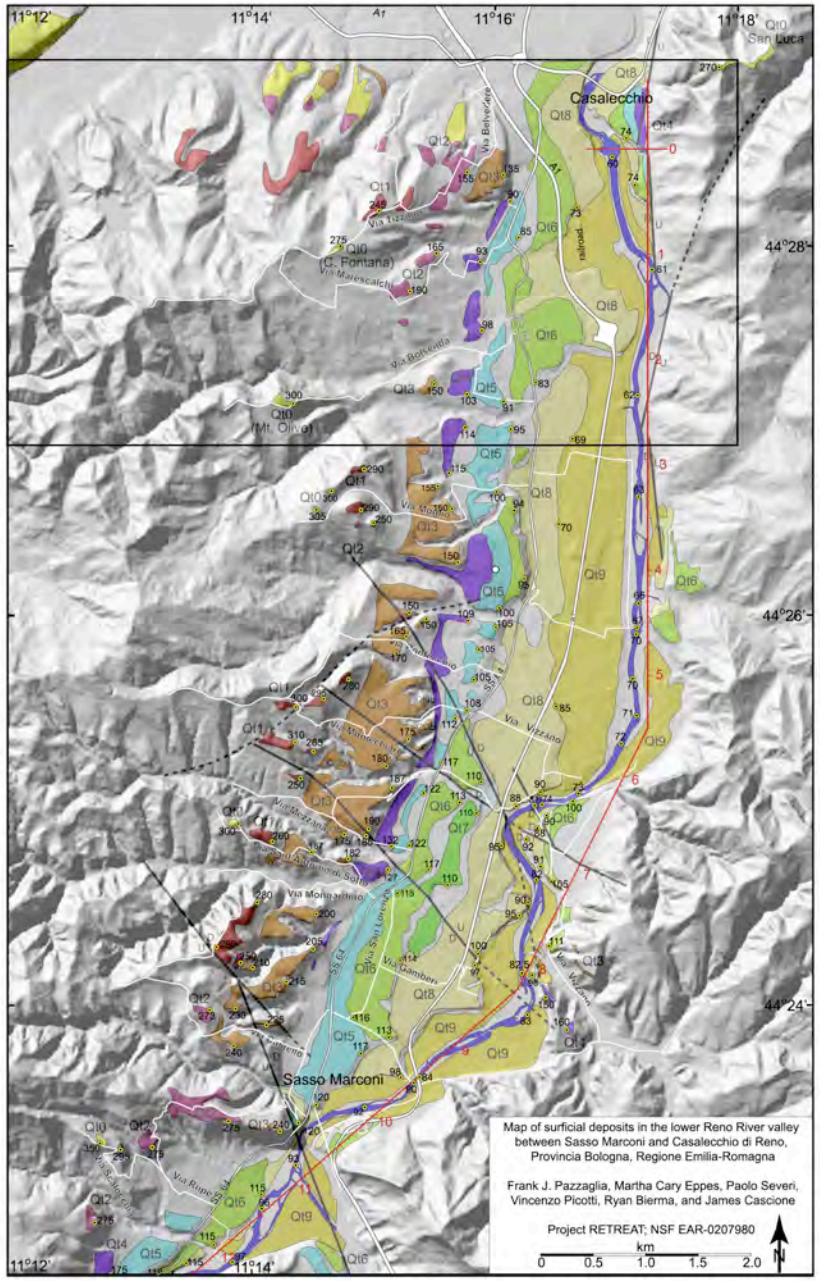

Figure 5. Map of terraces in the lower Reno valley between Sasso Marconi (south) and Casalecchio di Reno (north). Yellow points are elevations in meters. Topography in the black outline is used for the swath profile of Figure 6a. The red line is the valley plane profile to which all longitudinal profile data are projected in Figure 7. Terrace stratigraphy is illustrated in Figure 6 and Table 1.

Picotti and Pazzaglia 2008

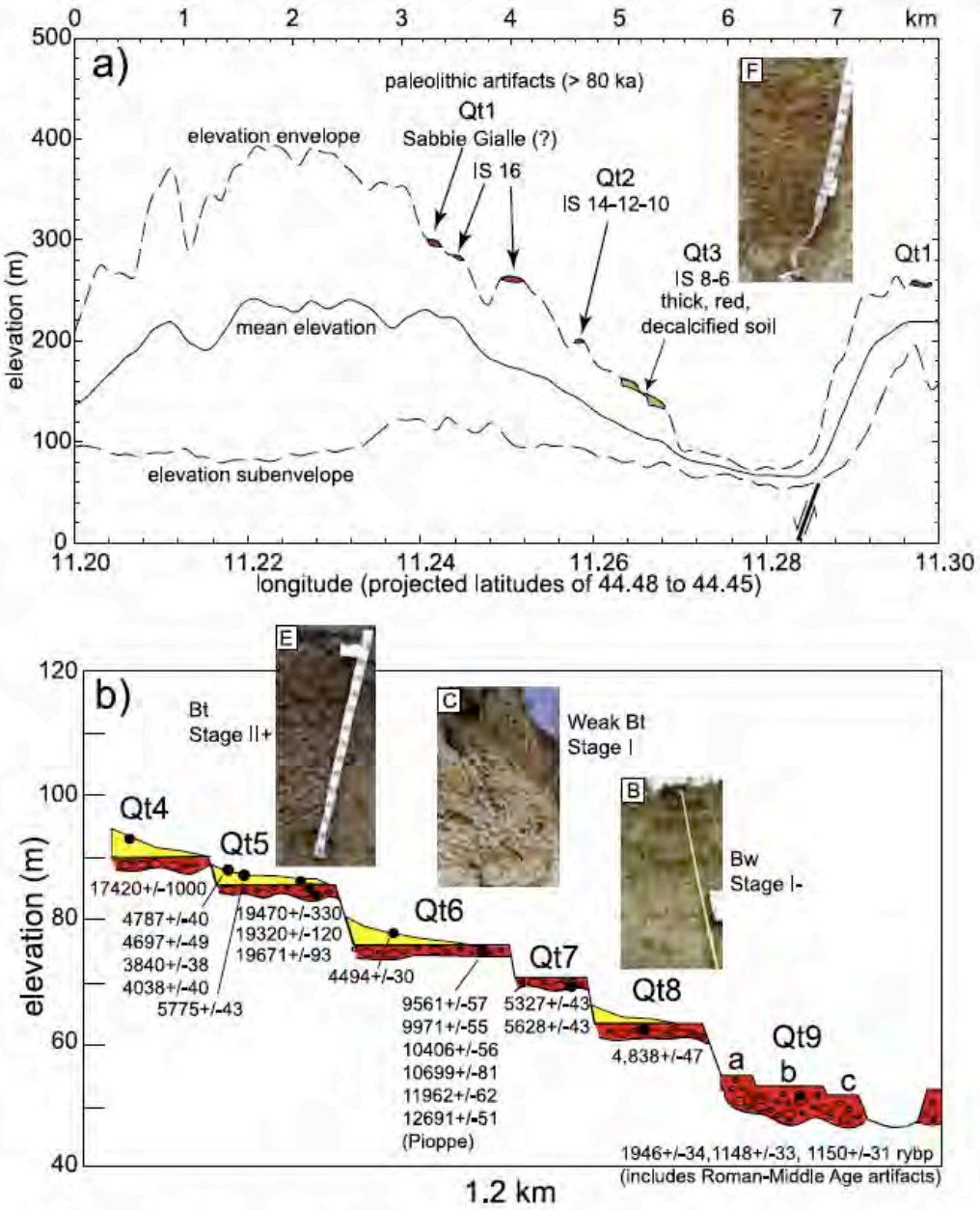

Figure 6. (a) Topographic swath profile of the lower Reno valley between latitudes 44.48 and 44.45 with terrace locations and inferred ages. (b) Composite cross-section of the inner Reno valley showing the late Pleistocene terraces and numeric ages. Red: alluvium; yellow: colluvium. Inset photographs of soils F, E, C, and B illustrate changes in relative weathering characteristics of the terrace deposits and are described in detail in *Epps et al.* [2008].

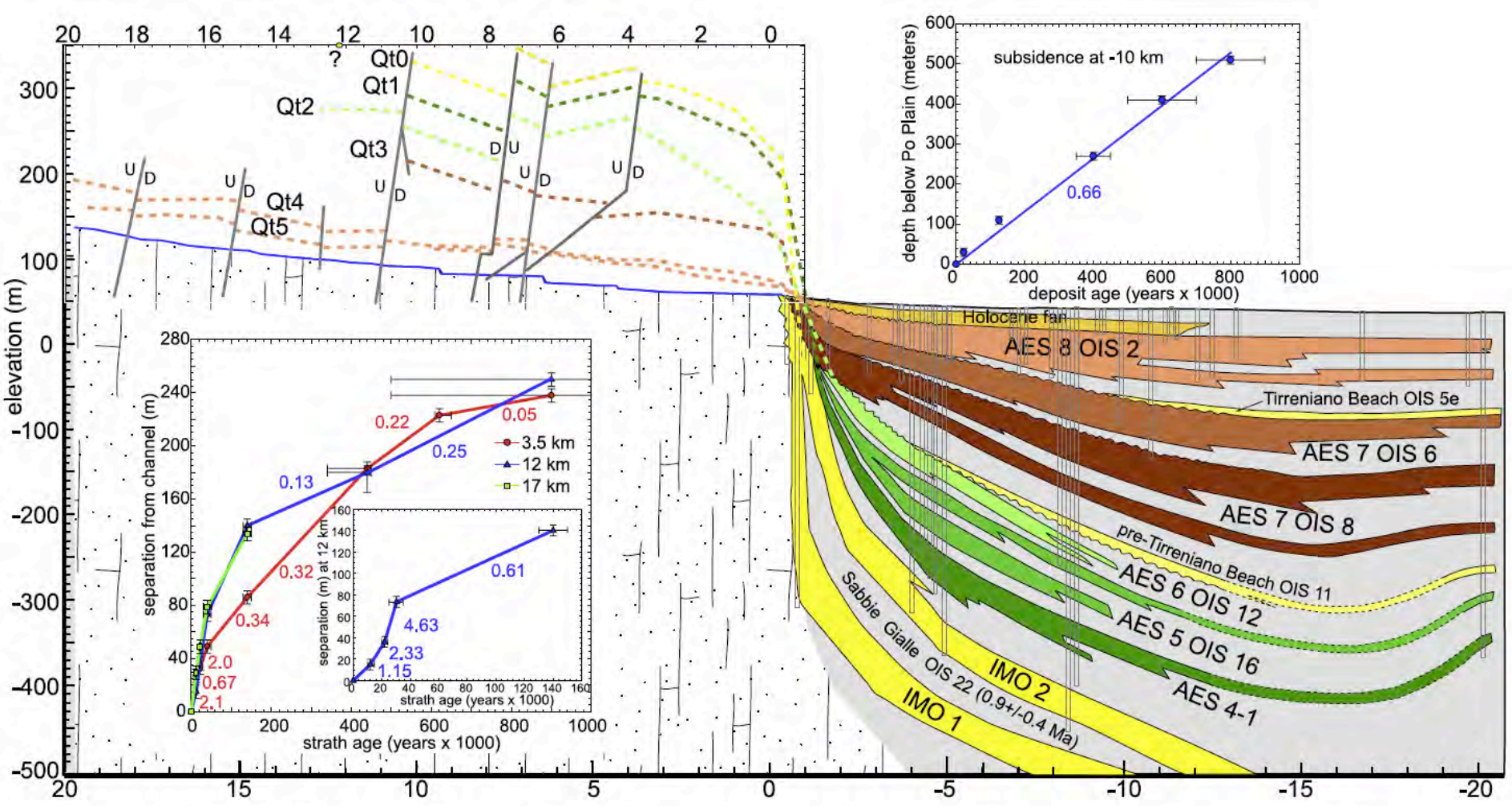

Figure 7. Projection and correlation of Reno terrace data across the mountain front to subsurface alluvial stratigraphy in the Po Plain. Numbers on inset graphs are incision or subsidence rates in millimeters per year. OIS, oxygen isotope stage, is used for stratigraphic correlation of deposits and terraces for which there exists no independent numeric ages. Age of IMO (Sabbie Gialle Qsg; cosmogenic; 0.9 ± 0.4 Ma) is from *Cyr and Granger* [2008].

Picotti and
Pazzaglia 2008

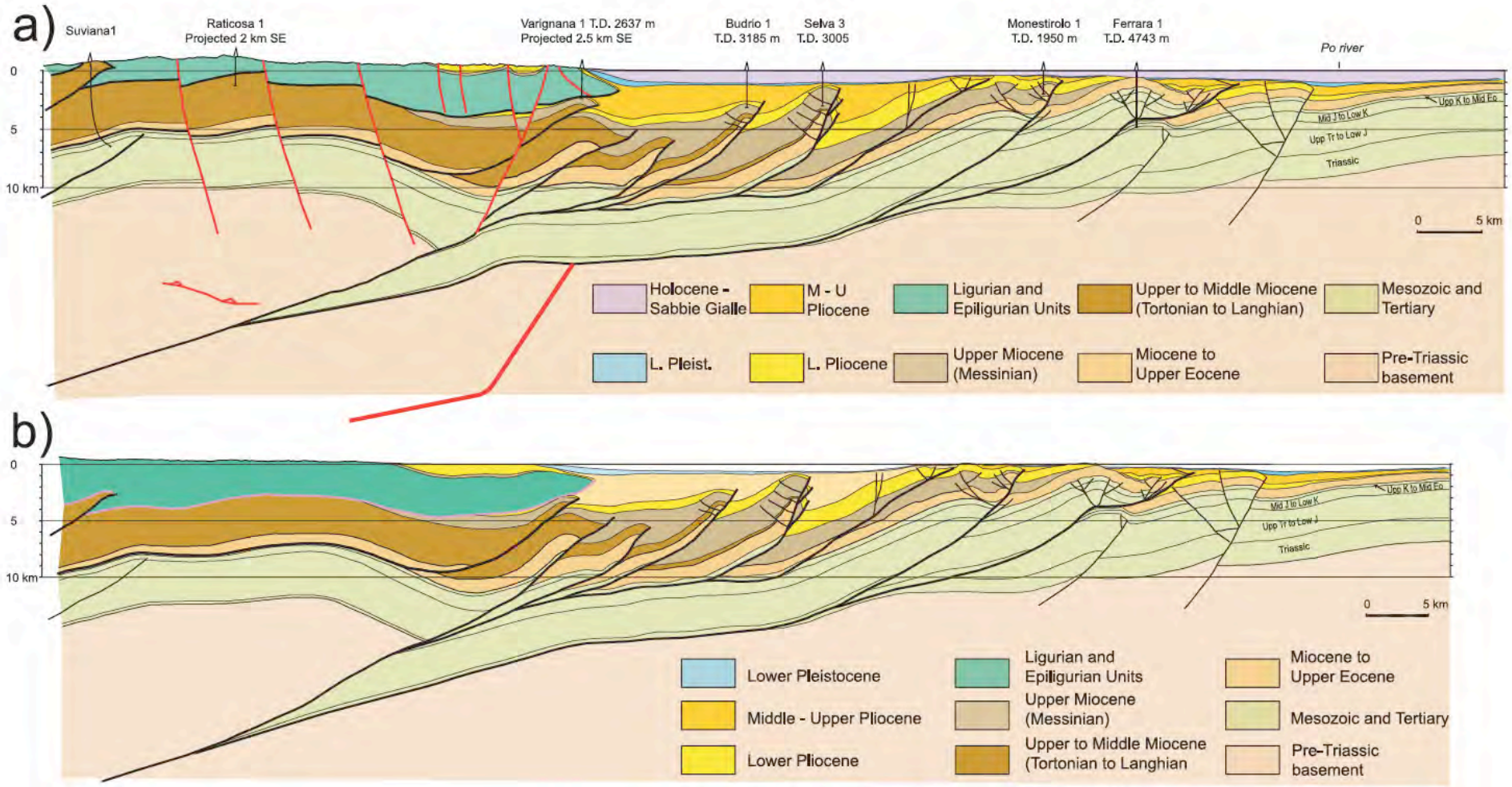

Figure 8. Geological cross-sections for (a) modern and (b) restored for the early Pleistocene. See Figure 4 for cross-section locations. The Po Plain portion comes from a reinterpretation of the seismic line C of *Pieri* [1987]; the Apennines transect comes from a reinterpretation of the cross-section IV of *Martelli and Rogledi* [1998]. The red lines in Figure 8a are active faults. The line denoting a fault in and out of the plane of the cross-section represents the Monghidoro earthquake [M 5.3, 2003; *Piccinini et al.*, 2006]. The deep ramp structure is inferred from modeling results of observed deformation and river incision (see Figure 9).

Picotti and Pazzaglia 2008

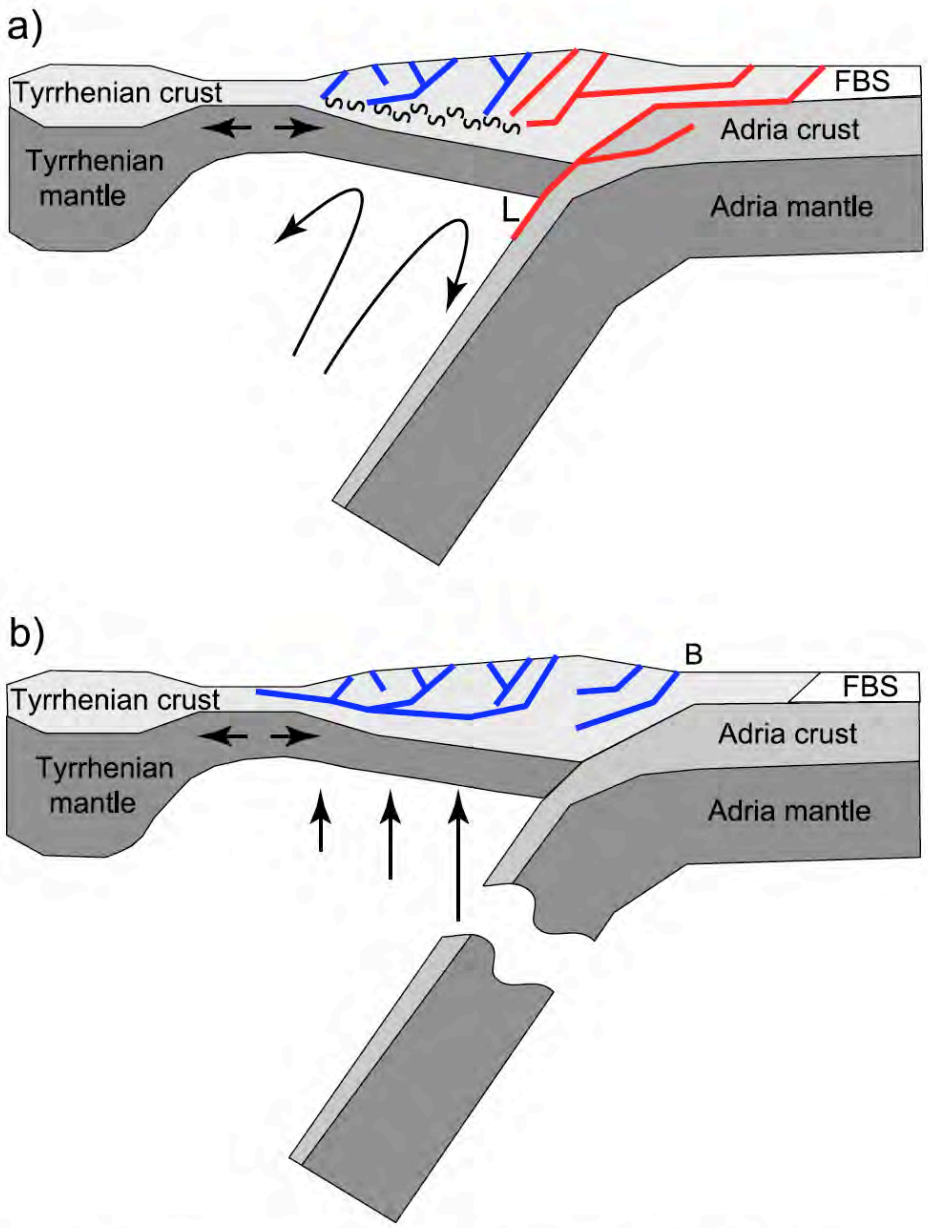

Figure 2. The two end-members for the Quaternary tectonics and geodynamics of the Apennines, defined by the degree of crust-mantle coupling that drives the extensional process. (a) Decoupled or partially coupled

Picotti and Pazzaglia 2008

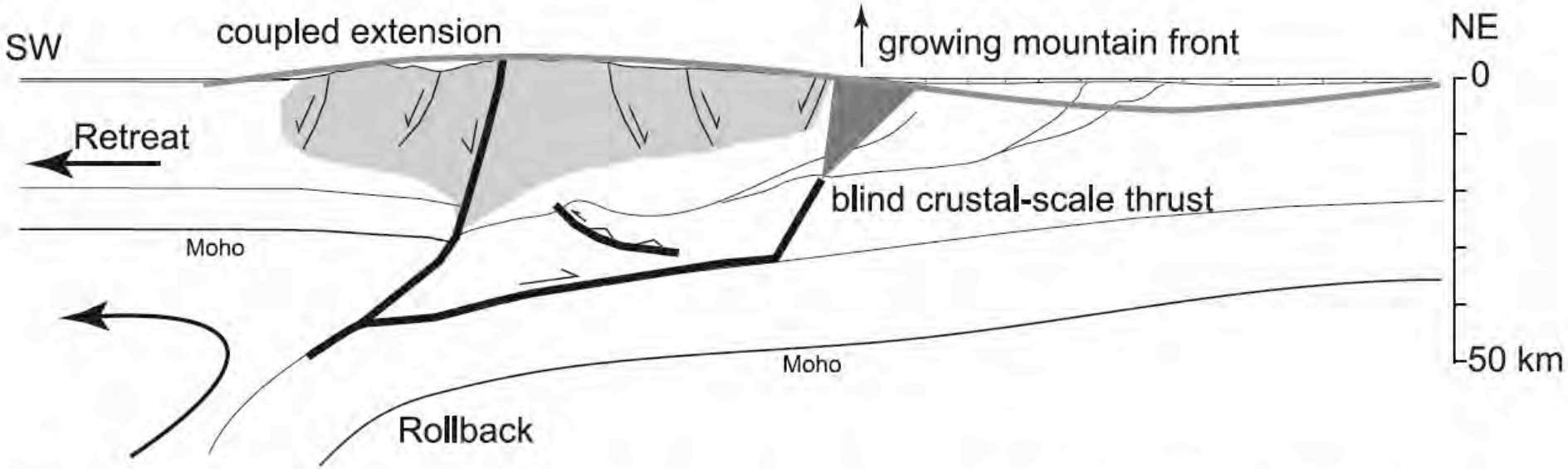

Figure 11. Active deformation of the northern Apennines in the context of a partially coupled rollback-retreat geodynamic model.

Picotti and Pazzaglia 2008

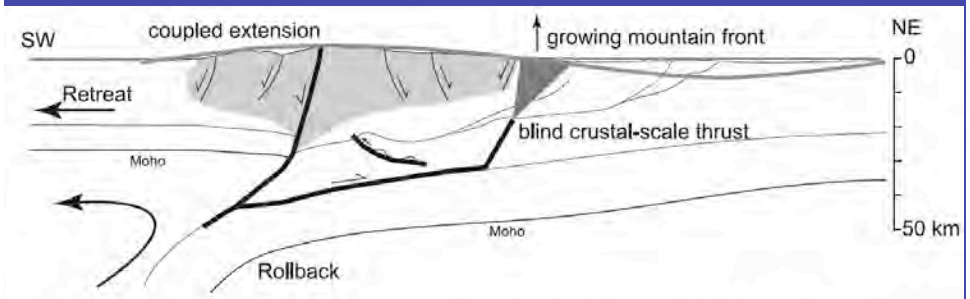

Figure 11. Active deformation of the northern Apennines in the context of a partially coupled rollback-retreat geodynamic model.

Picotti and Pazzaglia 2008

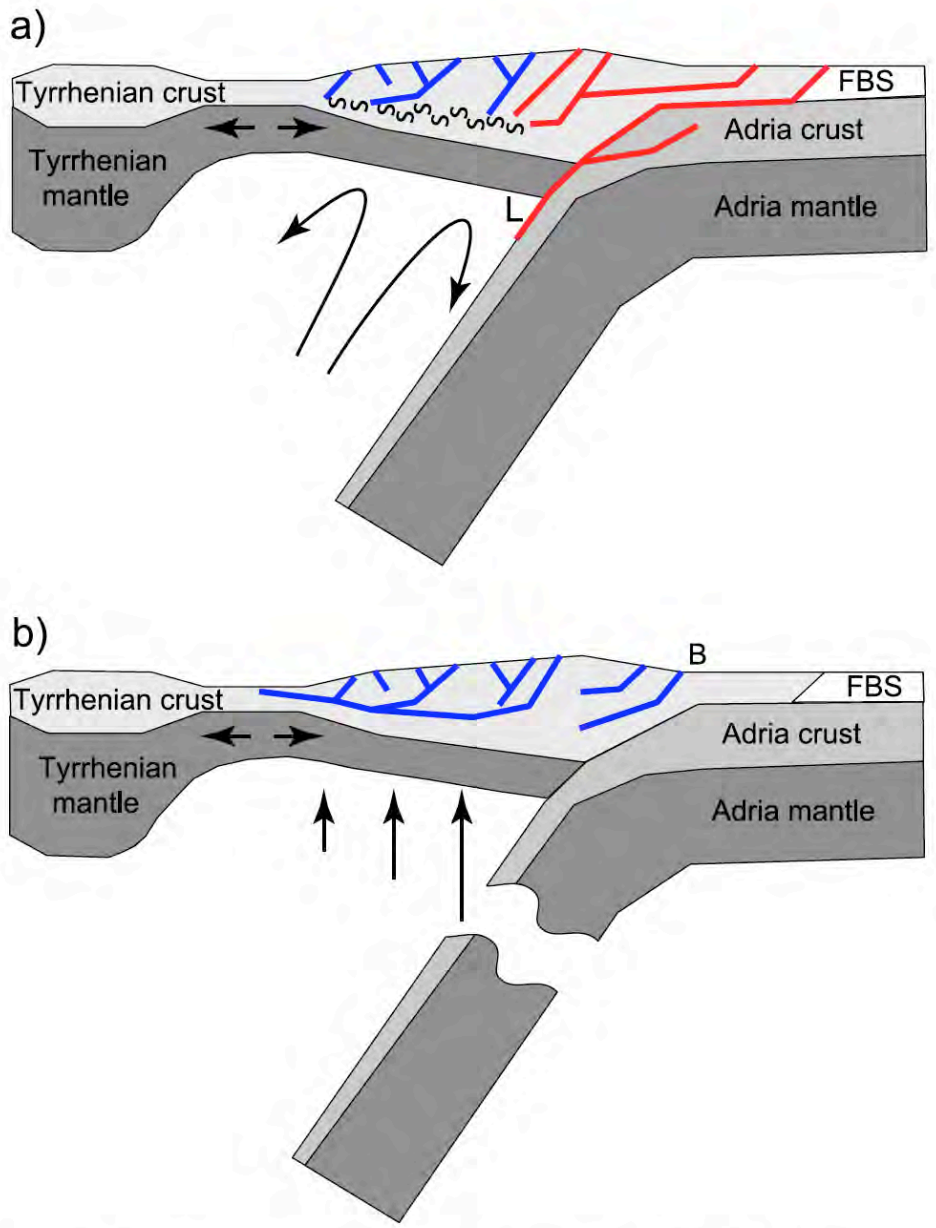

Figure 2. The two end-members for the Quaternary tectonics and geodynamics of the Apennines, defined by the degree of crust-mantle coupling that drives the extensional process. (a) Decoupled or partially coupled

Present

N Apennines

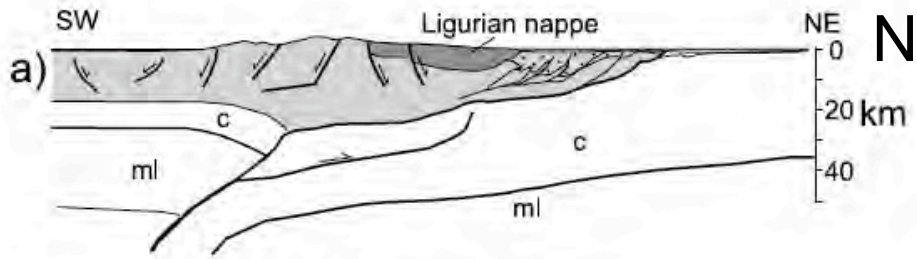

19 Ma

Central Alps

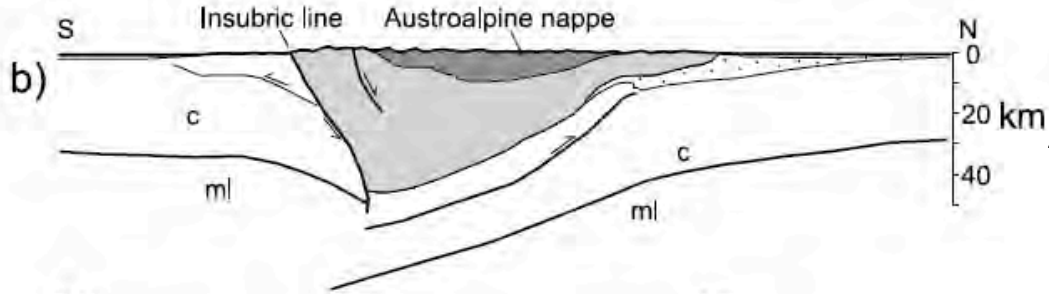

+20 Ma

N Apennines

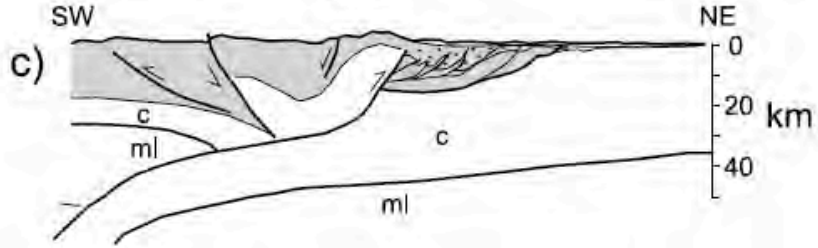

Present

Central Alps

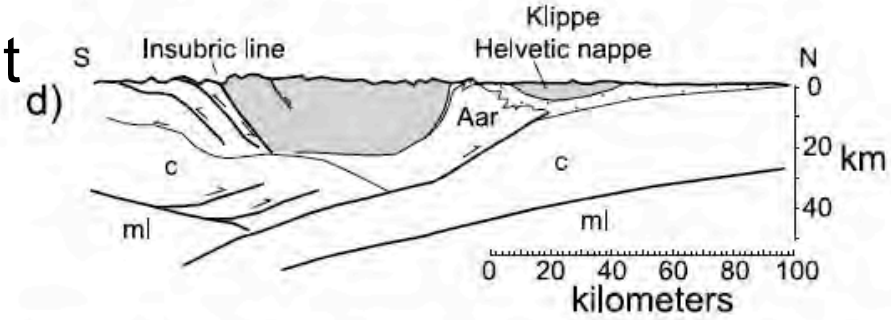

Figure 12. A comparison of the major tectonic features of the northern Apennines to the central Alps. (a) Northern Apennines at present; (b) central Alps 19 Ma; (c) northern Apennines 20 My into the future, with continued movement of the mountain front blind thrust fault; (d) central Alps at present, with the Aar Massif splitting the upper crustal orogenic wedge following shortening on a crustal-scale blind thrust. c, crust; ml, mantle lithosphere. Dark lines indicate active faults. Dots indicate proforeland deposits.

Picotti and Pazzaglia 2008